Title	Decreased anxiety-related behaviour but apparently unperturbed NUMB function in ligand of NUMB protein-X (LNX) 1/2 double knockout mice
Authors	Lenihan, Joan A.;Saha, Orthis;Heimer-McGinn, Victoria;Cryan, John F.;Feng, Guoping;Young, Paul W.
Publication date	2016-11-26
Original Citation	Lenihan, J. A., Saha, O., Heimer-McGinn, V., Cryan, J. F., Feng, G. and Young, P. W. (2016) 'Decreased anxiety-related behaviour but apparently unperturbed NUMB function in ligand of NUMB protein-X (LNX) 1/2 double knockout mice', Molecular Neurobiology, 54(10), pp. 8090-8109. doi:10.1007/s12035-016-0261-0
Type of publication	Article (peer-reviewed)
Link to publisher's version	10.1007/s12035-016-0261-0
Rights	© 2016, Springer Science+Business Media New York. The final publication is available at Springer via http://dx.doi.org/ 10.1007/s12035-016-0261-0
Download date	2025-03-21 23:16:18
Item downloaded from	https://hdl.handle.net/10468/3505

Decreased Anxiety-Related Behaviour but Apparently Unperturbed NUMB Function in Ligand of NUMB Protein-X (LNX) 1/2 Double Knockout Mice

Joan A. Lenihan, [1]

Orthis Saha, [1,2]

Victoria Heimer-McGinn, [1,3]

John F. Cryan, [4,5,6]

Guoping Feng, [7,8,9]

Paul W. Young, [1,*,64]

Phone +353 21 420 5994
Email p.young@ucc.ie

[1] School of Biochemistry and Cell Biology, University College Cork, Cork, Ireland

[2] Present Address: Institut de Biologie de l'ENS (IBENS), INSERM, CNRS, École Normale Supérieure, PSL Research University, 75005 Paris, France

[3] Present Address: Department of Cognitive, Linguistic and Psychological Sciences, Brown University, Providence, RI, USA

[4] Department of Anatomy and Neuroscience, University College Cork, Cork, Ireland

[5] Alimentary Pharmabiotic Centre, University College Cork, Cork, Ireland

[6] Cork Neuroscience Centre, University College Cork, Cork, Ireland

[7] McGovern Institute for Brain Research, Department of Brain and Cognitive Sciences, Massachusetts Institute of Technology, Cambridge, MA, 02139 USA

[8] Key Laboratory of Brain Functional Genomics (Ministry of Education and Science and Technology Commission of Shanghai Municipality), Institute of Cognitive Neuroscience, School of Psychology and Cognitive Science, East China Normal University, Shanghai, 200062 China

[9] Stanley Center for Psychiatric Research, Broad Institute of Massachusetts Institute of Technology and Harvard, Cambridge, MA, 02142 USA

Abstract

NUMB is a key regulator of neurogenesis and neuronal differentiation that can be ubiquitinated and targeted for proteasomal degradation by ligand of numb protein-X (LNX) family E3 ubiquitin ligases. However, our understanding of LNX protein function in vivo is very limited. To examine the role of LNX proteins in regulating NUMB function in vivo, we generated mice lacking both LNX1 and LNX2 expression in the brain. Surprisingly, these mice are healthy, exhibit unaltered levels of NUMB protein and do not display any neuroanatomical defects indicative of aberrant NUMB function. Behavioural analysis of LNX1/LNX2 double knockout mice revealed decreased anxiety-related behaviour, as assessed in the open field and elevated plus maze paradigms. By contrast, no major defects in learning, motor or sensory function were observed. Given the apparent absence of major NUMB dysfunction in LNX null animals, we performed a proteomic analysis to identify neuronal LNX-interacting proteins other than NUMB that might contribute to the anxiolytic phenotype observed. We identified and/or confirmed interactions of LNX1 and LNX2 with proteins known to have presynaptic and neuronal signalling functions, including the presynaptic active zone constituents ERC1, ERC2 and LIPRIN-αs (PPFIA1, PPFIA3), as well as the F-BAR domain proteins FCHSD2 (nervous wreck homologue) and SRGAP2. These and other novel LNX-interacting proteins identified are promising candidates to mediate LNX functions in the central nervous system, including their role in modulating anxiety-related behaviour.

Keywords

LNX1
LNX2
LIPRIN/PPFIA
ERC1/ERC2
NUMB
Anxiety

Abbreviations

PDZ	PSD-95
DlgA	ZO-1

RING	Really Interesting New Gene
LNX	Ligand of numb protein X
CNS	Central nervous system
ERC	ELKS/Rab6-interacting/CAST
SVZ	Subventricular zone
PBK	PDZ-binding kinase
DKO	$Lnx1^{exon3-/-}$;$Lnx2^{-/-}$ double knockout
DHET	$Lnx1^{exon3+/-}$;$Lnx2^{+/-}$ double heterozygous knockout
GFP	Green fluorescent protein
GST	Glutathione S-transferase
PCR	Polymerase chain reaction
PTB	Phosphotyrosine-binding domain

Electronic supplementary material

The online version of this article (doi: 10.1007/s12035-016-0261-0) contains supplementary material, which is available to authorized users.

Introduction

Ligand of NUMB protein X (LNX) proteins were first characterized based on their ability to bind to NUMB and NUMBLIKE [1, 2]. LNX1 and LNX2 are closely related E3 ubiquitin ligases that can ubiquitinate specific isoforms of NUMB, and LNX-mediated ubiquitination, at least in the case of LNX1, has been shown to target NUMB for proteasomal degradation [3, 4, 5]. NUMB is a negative regulator of Notch signalling, and degradation of NUMB upon LNX1 overexpression was shown to moderately enhance Notch signalling in cultured cells [4]. However, LNX2 knockdown in colorectal cancer cell lines caused a decrease in NUMB levels, a result that does not fit with the notion of LNX2 targeting NUMB for degradation [6]. Developmentally, expression of both *Lnx*1 and *Lnx2* messenger RNA (mRNA) is prominent in the embryonic and adult central nervous system (CNS) [1, 2]. This observation suggests a possible role for LNX1 and LNX2 in modulating neural development through their interaction with NUMB and/or its paralogue NUMBLIKE—key regulators of mammalian neurogenesis and neuronal differentiation [7]. However, LNX proteins are present at very low levels in the brain, despite the presence of *Lnx* mRNAs [8], and the regulation of NUMB by endogenous levels of LNX proteins has not been definitively demonstrated. One of many aspects of neural development regulated by NUMB/NUMBLIKE is the development of the neurogenic subventricular zone (SVZ) [9]. A recent study has reported an upregulation of LNX2 within

the SVZ of mice lacking the *Gli3* transcriptional repressor and demonstrated that these mice have lower levels of NUMB protein [10]. However, a causal relationship between these two observations was not proven and the question of whether NUMB is modulated by endogenous levels of LNX proteins in the SVZ has not been addressed. There have not been any in vivo *Lnx* loss-of-function studies in a mammalian context, and hence, the physiological significance of the LNX–NUMB interaction remains unclear.

LNX1 and LNX2 have the same domain structure, comprising an amino-terminal Really Interesting New Gene (RING) domain, a NUMB-binding motif (NPAY or NPAF) and four carboxyl-terminal PSD-95, DlgA and ZO-1 (PDZ) domains (Fig. 1). The RING domain harbours the catalytic E3 ubiquitin ligase activity, but notably, the shorter LNX1 p70 and p62 isoforms that are expressed in the brain lack the RING domain, suggesting that they might have functions that are independent of ubiquitination [1, 11]. No such alternative splicing of *Lnx2* has been reported. The combination of a RING and one or more PDZ domains is unique to the LNX family [12]. PDZ domains function as protein–protein interaction modules, most commonly binding to the carboxyl-termini of other proteins. Wolting et al. [13] catalogued around 220 LNX-interacting proteins both from their own work and the published literature, while a subsequent study by Guo et al. [14] added approximately 30 additional proteins to this list. Most of these interactions are PDZ domain-mediated and were identified using either yeast two-hybrid assays or arrays of PDZ domains and PDZ-binding motifs. To date, only a small number of the described LNX-interacting proteins have been shown to be substrates for ubiquitination by LNX. For example, ubiquitination of c-Src and PDZ-binding kinase (PBK) by LNX1 targets them for proteasomal degradation [8, 14], while LNX-mediated ubiquitination of CLAUDINS and CD-8α appears to cause their internalization from the cell surface, via endocytic pathways [15, 16]. Nevertheless, these examples indicate that the ubiquitin ligase activity of LNX proteins can be targeted to specific substrates via PDZ-mediated interactions. Thus, we need to consider interacting proteins beyond NUMB and NUMBLIKE that may be substrates for ubiquitination by LNX proteins or that may mediate E3 ligase-independent LNX functions. Given the low and potentially cell type-restricted expression patterns of LNX proteins [8, 11, 17], the identification of physiologically relevant interacting proteins and substrates will be key to elucidating the in vivo functions of LNX proteins.

Fig. 1

Generation of *Lnx1*$^{exon\ 3}$*;Lnx2* double knockout (DKO) mice. **a** Schematic of *Lnx1* gene structure showing the alternative promoters (*large arrows*) and splicing events (*thin lines*) that generate the non-neuronal p80 and the neuronal p70 and p62 protein isoforms. In the knockout allele, exon 3, the first exon of all the

neuronal transcripts, is deleted and replaced by a neomycin resistance cassette. *Arrowheads* show the locations of translation initiation ATG codons for the indicated protein isoforms. *Small arrows* in **a**, **b** indicate positions of genotyping primers. **b** Schematic of *Lnx2* wild-type, floxed and knockout alleles. Exon 2, which contains the ATG codon for the initiation of LNX2 translation, was first flanked by *loxP* sites and then deleted through Cre-mediated recombination to generate the knockout allele used in this study. HindIII restriction sites are indicated by the letter *H*, and the *grey bar* indicates the probe used for southern blotting (not to scale). **c**, **d** Domain structures of LNX1 and LNX2 proteins. The LNX1 p70 and p62 isoforms that lack the catalytic RING domain are expressed in the central nervous system. The NPAY and NPAF motifs in LNX1 and LNX2 respectively are involved in binding NUMB while both proteins contain four PDZ domains. **e** Southern blot verifying correct *Lnx2* gene targeting. A HindIII restriction site in the targeting construct results in a shorter 5.5-kb fragment being generated upon HindIII digestion of genomic DNA from three correctly targeted ES cell clones (*1*, *2*, *3*), compared to the parental ES cells (*C*). **f** PCR-based genotyping of wild-type (*WT*), $Lnx1^{exon3+/-}/Lnx2^{+/-}$ (*DHET*) and $Lnx1^{exon3-/-}/Lnx2^{-/-}$ (*DKO*) mice analysed by agarose gel electrophoresis. Using the primer pairs indicated in **a**, **b** above, *Lnx1* and *Lnx2* WT and KO alleles were detected in separate PCR reactions. **g**, **h** Elimination of LNX1 and LNX2 proteins from the brains of *Lnx1/Lnx2* DKO mice confirmed by western blotting of brain lysates (*left panels*) and immunoprecipitates (*right panels*) from WT and DKO mice. Immunoprecipitation was performed using an antibody that recognizes both LNX1 and LNX2. **g** Immunoblotting using an anti-LNX1 antibody that cross reacts with LNX2 does not detect LNX proteins directly in brain lysates at any of the indicated developmental stages. However, following immunoprecipitation, neuronal LNX1p70 and p62 isoforms as well as LNX2 (75 kDa) are all detected in WT, but not DKO, P18 brains. **h** Immunoblotting using a LNX2-specific antibody directly detects LNX2 in WT, but not DKO, E14.5, P1 and P7 brain lysates. LNX2 cannot be clearly detected by immunoblotting at P18 or adult (P42) stages without prior immunoprecipitation. In P1 mice, LNX2 is present across multiple brain regions. The positions (or expected positions) of LNX proteins (*arrows*) as well as molecular weight markers (kDa) are indicated. *Asterisks* (*) indicate non-specific bands. *Ad* adult, *Olf B* olfactory bulb, *Fore Br* forebrain, *Mid Br* Midbrain, *Br Stm* brain stem, *Cereb* cerebellum, *Sp Cord* Spinal Cord

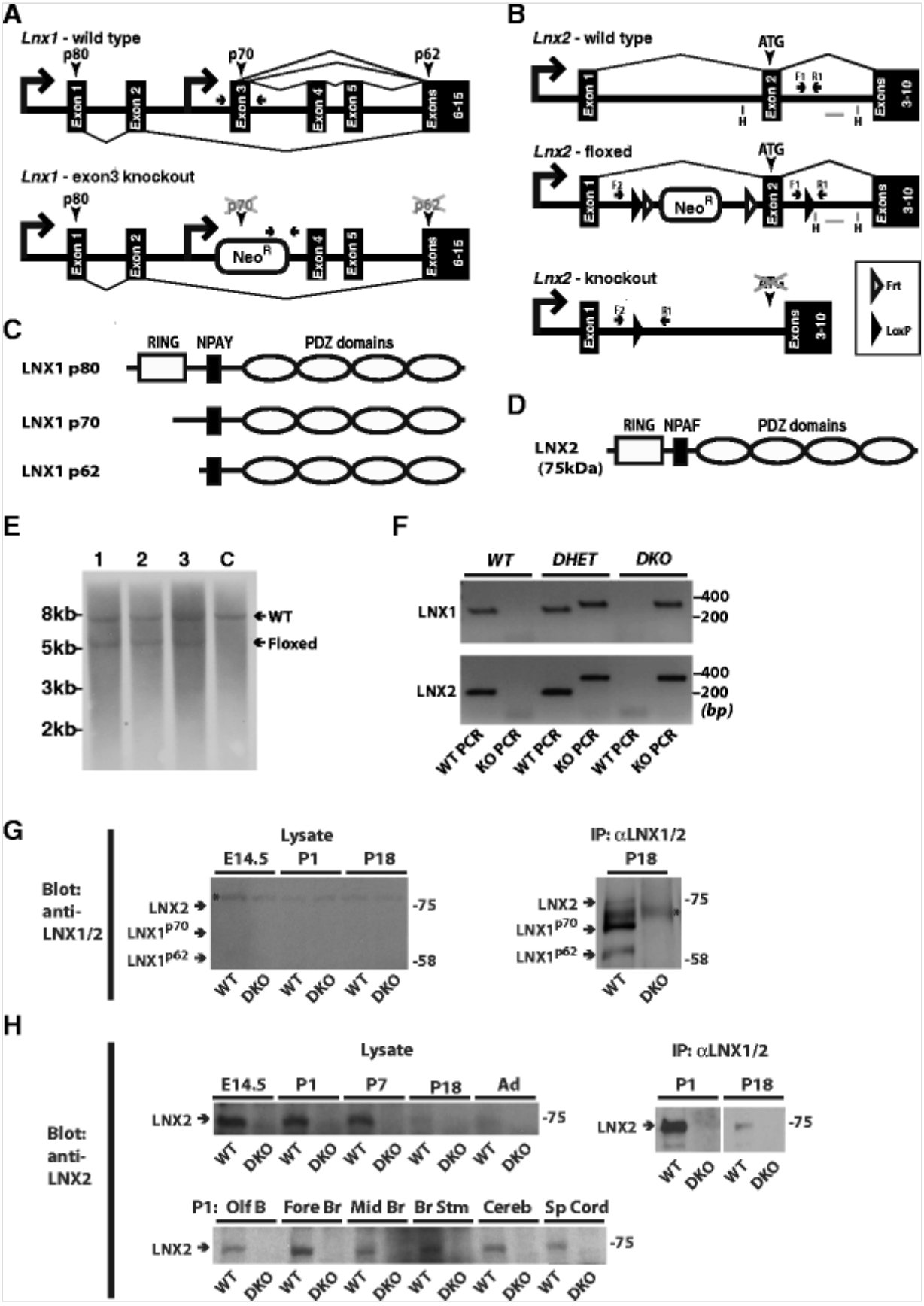

To explore the neuronal functions of LNX proteins in vivo, we generated double knockout mice that lack LNX protein expression in the CNS. These mice exhibit decreased anxiety-related behaviours, in the apparent absence of any sensory, motor or learning deficits. However, we do not find evidence to support the hypothesis that LNX proteins are major regulators of NUMB/NUMBLIKE

function during CNS development. To identify other proteins that may mediate LNX functions in the CNS, we characterized brain proteins that bind LNX1 and LNX2 PDZ domains using affinity purification and mass spectrometry. This approach revealed interactions of LNX1 and LNX2 with proteins that have established synaptic or neuronal functions, including ERC1/ERC2, LIPRIN-αs, FCHSD2 and SRGAP2—providing candidates in addition to NUMB that may play a role in the altered anxiety-related behaviour in LNX-deficient mice.

Materials and Methods

Animals

Lnx1$^{exon3-/-}$ knockout mice (originally made by Lexicon Pharmaceuticals, Inc.) were obtained through the Mutant Mouse Regional Resource Center (MMRRC, www.mmrrc.org) at University of California, Davis, CA, USA (stock no. 032436-UCD; strain name: B6;129S5-Lnx1<tm1Lex>/Mmcd). In these mice, exon 3, which is the first exon of the transcripts that codes for the p70 and p62 neuronal isoforms of LNX1, is replaced by a neomycin resistance gene (Fig. 1a). This is expected to abolish transcription of these neuronal isoforms, but should not affect the expression of the non-neuronal LNX1 p80 isoform that is transcribed from a different upstream promoter [11].

Lnx2 conditional knockout mice were generated through homologous recombination in mouse R1 embryonic stem (ES) cells by using standard procedures as previously described [18]. These *Lnx2* conditional knockout mice were designed so that a neomycin resistance gene, used as a selectable marker, and the adjacent exon 2 of the *Lnx2* gene are flanked by *loxP* sites (Fig. 1b). Exon 2 and the neomycin resistance gene were deleted by crossing these mice to a Cre recombinase-expressing transgenic mouse line from the Jackson Laboratory, Bar Harbor, ME, USA (strain name: B6.C-Tg(CMV-cre)1Cgn/J; stock no. 006054). The heterozygote (*Lnx2*$^{+/-}$) mice, so obtained, were then crossed with each other to obtain knockout (*Lnx2*$^{-/-}$) mice. Removal of exon 2 deletes the ATG start codon and the coding region for the RING finger domain. If, following deletion of exon 2, exon 1 were to splice into exon 3 or a downstream exon, and the first available in-frame ATG (in exon 7) was used to initiate translation, a protein of 211 amino acids in length could theoretically be produced. However, several out-of-frame ATGs in exons 3–6 would likely attenuate translation of any such product. Thus, deletion of exon 2 in *Lnx2* is likely to result in the production of at most very small quantities of a severely truncated LNX2 polypeptide lacking E3 ligase activity and is highly likely to be a null or severely hypomorphic allele.

AQ1

Lnx2$^{-/-}$ mice were crossed to *Lnx1*$^{exon3-/-}$ mice. Compound heterozygous mice *Lnx1*$^{exon3+/-}$ and *Lnx2*$^{+/-}$ were obtained and back-crossed for at least eight generations to the C57/BL6J strain to ensure a uniform C57/BL6J genetic background. After back-crossing, double knockout (DKO) mice (*Lnx1*$^{exon3-/-}$;*Lnx2*$^{-/-}$) and the other genotypes required were bred for the experiments described hereafter. All animal experiments were approved by the Animal Experimentation Ethics Committee of University College Cork (No: 2013/028) and were conducted under licence (No: AE19130/P013) issued by the Health Products Regulatory Authority of Ireland, in accordance with the European Union Directive 2010/63/EU for animals used for scientific purposes.

AQ2

Genotyping

Tail biopsies were digested with Proteinase K as described previously [19]. PCR genotyping was performed using the following cycling conditions: 96 °C—3 min, 40 cycles [96 °C—40 s, 60 °C—40 s, 68 °C—1 min 30 s] and 68 °C—10 min. Primer pairs and sizes of PCR products were as follows:

- *Lnx1* WT PCR—DNA274-3 [5′-TGCCTTAATCTACAGGCTCC-3′] and DNA274-4 [5′-GAGTTGTGGGCACTGAGAG-3′], 253 bp
- *Lnx1* KO PCR—Neo3a 5′ [5′-GCAGCGCATCGCCTTCTATC-3′] and DNA274-7 5′ [5′-GTCACAAAGCACTAAGCGTG-3′], 298 bp
- *Lnx2* WT/FLOX PCR—*Lnx2*GENO-F1 [5′-CGCAGCCTTAGGCATGGTTGG-3′] and *Lnx2*GENO-R1 [5′-CTGACTGTGGGTTACAGTTCTGG], 210 /252 bp
- *Lnx2* KO PCR—*Lnx2*GENO-F2 [CCCCATCATGCAGAGCAAAGTC] and *Lnx2*GENO-R1, 368 bp

Antibodies and cDNA Constructs

The coding sequences of mouse *Lnx1* (p80 isoform) and *Lnx2* were cloned into the pEGFP-C2 vector (Clontech, Mountain View, CA, USA). Empty pEGFP-C2 vector was used to express EGFP alone. Constructs encoding the second PDZ domains of LNX1 and LNX2, corresponding to aa377–470 and aa330–423 respectively, were cloned into the vector pET24d-GST to produce glutathione S-transferase (GST)-tagged proteins. Coding sequences for LNX-interacting proteins were cloned into the vector pCMV-N-FLAG to produce proteins with amino-terminal FLAG epitope tag. The following commercially available antibodies were used at the indicated dilutions: anti-green fluorescent protein

(GFP, catalogue number ab290, Abcam, 1:3000 dilution), anti-FLAG (catalogue number F3165, Sigma-Aldrich, 1:15,000 dilution), anti-LIPRIN-α3 (catalogue number 169102, Synaptic Systems, 1:1000 dilution), anti-NUMB (catalogue number NB500-178, Novus Biologicals, 1:7000 dilution), anti-FOXJ1 (catalogue number 14-9965, e-Bioscience, 1:400 dilution), anti-glial fibrillary acidic protein (GFAP, catalogue number ab7260, Abcam, 1:1000 dilution) and anti-VINCULIN (catalogue number V9131, Sigma-Aldrich, 1:1000 dilution). The guinea pig polyclonal anti-LNX1/2 antibody (anti-LNX1/2-PDZ3/4), rabbit anti-LNX2 antibody (used at 1:500 dilution) [17] and the rabbit polyclonal anti-LNX1/2 antibody (anti-LNX1/2-RING/NPAY, used at 1:3000 dilution) [1] have been described previously. Secondary antibodies were from Jackson ImmunoResearch Laboratories (West Grove, PA, USA) and LI-COR Biosciences (Cambridge, UK). All reagents were from Sigma-Aldrich (Arklow, Ireland) unless stated otherwise.

Western Blotting and Immunoprecipitation

Brain tissues from wild-type (WT) and DKO mice were homogenized on ice using a Dounce homogenizer in a volume of lysis buffer (20 mM, pH 7.5, 10 mM NaCl, 1% NP40, 0.1% sodium deoxycholate, 1 mM EDTA and protease inhibitors (Roche Applied Sciences)) which was 10 times the weight of the tissue. Following centrifugation at 16,000×*g* for 30 min at 4 °C, the supernatants were used directly either for western blotting (to detect NUMB or LNX proteins) or for immunoprecipitation of LNX proteins. Immunoprecipitation was performed on lysates prepared from approximately 0.4 g of brain tissue, by addition of 10 µl guinea pig anti-LNX1/2-PDZ3/4 serum [17] for 4 h and 50 µl Protein A sepharose beads (Thermo Scientific Pierce) for 2 h with mixing at 4 °C. Following 5 × 5 min washes in lysis buffer, immunoprecipitated proteins were eluted by boiling in 2× SDS-PAGE gel loading buffer. Western blotting for LNX proteins was performed using rabbit anti-LNX1/2-RING/NPAY or anti-LNX2 antibody and enhanced chemiluminescent detection (Thermo Scientific Pierce, Rockford, IL, USA). For NUMB quantification, total protein concentration of lysates was calculated using a BCA assay (Thermo Scientific Pierce) and NUMB detection was performed using Odyssey V2.1 software (LI-COR Biosciences, Cambridge, UK).

Histology and Immunofluorescence Staining

Mice to be used for histology and immunofluorescence were anesthetized by isofluorane inhalation and perfused transcardially with phosphate-buffered saline (PBS) followed by 4% paraformaldehyde dissolved in PBS. To examine gross brain anatomy, 66-µm-thick sagittal brain sections were cut using a vibratome and stained with DAPI dissolved in PBS in a 24-well plate with rocking, washed

three times for 10 min in PBS sections prior to mounting with Fluoromount mounting solution. Images were captured and montages of entire sections created using an EVOS FL Cell Imaging System microscope and associated software (Thermo Scientific Pierce). Brain regions were identified with the aid of the Allen Brain Atlas (http://mouse.brain-map.org) and quantified using ImageJ software [20]. For immunofluorescence staining, fixed tissues were cryoprotected in sucrose before embedding and freezing in OCT compound (Tissue-Tek, Torrance, CA, USA). Twenty-micrometre cryostat sections were fixed post sectioning with 4% paraformaldehyde/PBS for an additional 5 min, rinsed extensively with PBS and then blocked with blocking solution (2% bovine serum albumin (BSA), 5% normal goat serum (NGS) and 0.2% Triton X-100 diluted in PBS). Antibody incubations were performed at 4 °C overnight in blocking solution lacking Triton X-100. Sections were mounted with Fluoromount mounting solution and imaged on a Leica DM 6000 microscope. For FOXJ1 staining, antigen retrieval was performed in 10 mM Na citrate buffer (pH 6) for 20 min at 90–100 °C prior to the blocking step.

Phenotypic Characterization of Lnx DKO Mice

Mice were bred to obtain WT, double heterozygote (DHET) and DKO genotypes. Fathers were removed before parturition after which mothers were singly housed with their pups. Pups were weaned at 3 weeks of age and group-housed in groups of two to four mice of mixed genotype and fed ad libitum. Body weight was measured on a weekly basis to the nearest 0.1 g, beginning at 1 week of age. Cages contained minimally enriched living conditions, and mice were maintained on a 12-h light/dark cycle (lights on at 07:30), with temperature- (22 ± 1 °C) and humidity-controlled conditions. At adulthood (8 weeks old), mice underwent a battery of behavioural tests. Each cohort of mice, of a given sex and genotype, was made up of animals from at least three different litters. Tests were conducted in sequence from the least to the most stressful test, over a period of 5 weeks (Fig. 4a). There was a minimum rest period of at least 24 h between each test. For all procedures, animals were brought to the room at least 30 min prior to testing. All experiments were conducted during the light phase of the day. All apparatus were cleaned between animals with 70% ethanol to remove odours. Genotypes were blinded for the duration of the behavioural battery and for subsequent scoring.

Primary Observation, Grip Strength and Hotplate Tests

A primary observational assessment following a modified SHIRPA protocol was performed for male and female mice of each genotype [21, 22, 23]. In total, 36 observations were quantified, including spontaneous activity, respiration rate, fur, skin and whisker condition, tremor, body position, palpebral closure,

piloerection, gait, pelvic elevation, tail elevation, touch escape, positional passivity, transfer arousal, trunk curl, limb grasping, body tone, pinna reflex, corneal reflex, tail pinch reflex, skin colour, heart rate, limb tone, abdominal tone, lacrimation, provoked biting, righting reflex and negative geotaxis. In addition, muscle strength was assessed using a grip strength meter (Ugo Basile, Varese, Italy). Mice were held by the tail and brought allowed to grasp the grid with their front paws and were gently pulled back until they released their grip. The apparatus registered the peak strength for that trial. Each animal had five trials, with an inter-trial interval of 15–30 s. Mice were tested for analgesia-related responses using a hotplate apparatus preheated to 55 °C (Columbus Instruments, Columbus, OH, USA). Mice were placed onto the hotplate, and the time to first show a hind limb response was recorded. Typical responses are licking or shaking the hindpaw, or jumping. Mice were immediately removed after showing a response. The test was terminated at 30 s in the absence of a response.

Open Field

Spontaneous locomotor activity and anxiety-like behaviour were assessed in the open field task. This paradigm is based on the idea that mice will naturally prefer to be near a protective wall rather than being exposed to danger out in the open [21]. The apparatus was a grey, plastic, open box without any bedding (40 cm × 32 cm × 25 cm, $L \times W \times H$). The experiment was performed under dim light (circa 30 lx). After 30 min habituation to the testing room, animals were placed individually in the middle of the arena and allowed 10 min free exploration. Each mouse was video-recorded for the duration of the test, and the researcher left the room after the start of the trial. Total distance travelled, time spent and number of entries into the centre and the four corner areas of the arena were measured post-test using a video-tracking system (EthoVision software, Noldus, The Netherlands). The total distance travelled served as an index of locomotor activity. Time spent in the centre and number of entries into the centre and corners zones were considered an inverse score for anxiety-like behaviour.

Elevated Plus Maze

The elevated plus maze protocol is designed to test levels of passive anxiety-like behaviour, based on the conflict between the exploratory instinct of mice and their aversion for the elevated, exposed open arms of the maze [24]. The elevated plus maze consisted of four arms, forming the shape of a plus, elevated 91 cm above the floor. Two opposing arms were enclosed by walls; the other two arms were open. All four arms were connected by a centre area. The experiment was performed under dim light (circa 30 lx). Each mouse was placed gently on the centre of the maze facing an open arm and allowed to freely explore the

maze for 6 min. Each mouse was video-recorded for the duration of the test, and the researcher left the room after the start of the trial. Variables measured manually post-test were the time spent and percentage of entries into the open and closed arms of the maze, as indices of anxiety-like behaviour. Total arm entries were analysed as an index of general locomotor activity. An animal was adjudged to have entered an arm of the maze only when all four paws were inside the arm in question.

Light–Dark Box Test

The light–dark box test assessed levels of unconditioned anxiety in rodents based on levels of passive avoidance behaviour [24]. The apparatus was a plexiglas enclosure (44 cm × 21 cm × 21 cm, $L \times W \times H$) divided unequally into two chambers by a black partition containing a small opening (10 cm × 5 cm). The larger chamber was approximately twice the size of the smaller chamber, had clear walls and an open top and was brightly illuminated (1000 lx) to generate aversive conditions. The small chamber (14 cm length) was enclosed on all sides by black walls except for the small opening between the chambers. Mice were individually placed into the illuminated side facing away from the dark compartment and were allowed to freely explore the apparatus for 10 min. During this period, the behaviour of the animals was recorded. Mice were manually scored post-test for their initial latency to enter the dark compartment, the time spent in the light compartment and the number of transitions between the two compartments, using the recorded videos. An animal was adjudged to have entered a compartment when all four paws had crossed the threshold.

Y-Maze

Spontaneous alternation behaviour in the Y-maze is used to assess spatial memory [25]. The maze consisted of a black plastic three-arm Y-maze (15 cm × 5 cm × 10 cm, $L \times W \times H$). Mice were individually placed in one of the three arms and allowed 5 min free exploration. The sequence of visited arms was recorded. At the end of the test, mice were returned to their home cage. Parameters measured included the number of entries, as an index of locomotor activity, and the percentage alternation as a measure of spatial memory.

Rotarod Test

Motor coordination and skill learning were assessed using a rotarod apparatus (UGO Basile, Varese, Italy) [21]. The rotarod task was first introduced to animals by a 5-min trial at a constant speed of 4 rpm. During this initial training phase, mice were placed back on the rod immediately after falling, allowing them to become familiar with the test. Thereafter, mice were placed on the rotating drum, which accelerated from 4 to 40 r.p.m. over a 5-min period. Time

spent walking on top of the rod before falling was recorded. Mice were given three trials on three consecutive days for a maximum time of 300 s (5 min) per trial. An interval of 30 min was given between trials.

Other Behavioural Tests

As indicated in Fig. 4a, a number of additional behavioural tests were performed, the results of which are not presented here. Gait was monitored by analysis of paw print patterns, the acquisition and extinction of contextual and auditory cued fear was assessed in a fear conditioning paradigm and the forced swim test was performed as a measure of behavioural despair. No significant phenotypes were observed in these tests; however, for the latter two tests, which were performed at the end of the overall testing sequence, the possibility that the animals have become overly experienced to testing needs to be considered. The novel object recognition test was also performed; however, the data from this test could not be analysed because mice of all genotypes failed to preferentially explore the ‘novel’ objects used.

Purification of LNX1-PDZ2- and LNX2-PDZ2-Interacting Proteins from Brain Lysates

To prepare brain lysates, 0.8 g of brain tissue from P16 mice was resuspended in 2.5 volumes (*w*/*v*) of lysis buffer (10 mM Tris/Cl, pH 7.5, 150 mM NaCl, 0.5 mM EDTA, 0.5% NP-40 and protease inhibitors (Roche Applied Sciences)). After homogenization using a Dounce homogenizer, the samples were incubated on ice for 30 min with frequent agitation. Samples were then clarified by centrifugation at 16 000×*g* for 30 min at 4 °C. The supernatant was collected and diluted to a final volume that was 10 times the weight of the tissue in lysis buffer lacking NP-40. GST, GST-LNX1-PDZ2 and GST-LNX2-PDZ2 recombinant proteins were produced in *Escherichia coli* BL21 cells and purified with glutathione-sepharose 4B beads (GE Healthcare) as previously described [26]. Proteins were dialysed into binding buffer (20 mM Tris, pH 7.5, 50 mM NaCl, 5 mM β-mercaptoethanol), and 300 μl of GST or GST fusion protein at a concentration of 58 μM was added to 1 ml of brain lysate and incubated with mixing for 90 min at 4 °C. Forty microlitres of glutathione-sepharose beads was added, incubated for 10 min at 4 °C with rotation and washed three times in binding buffer for 5 min each at 4 °C. Bound proteins were eluted in 10 mM glutathione and 50 mM Tris/Cl, pH 8. Purified samples were prepared for mass spectrometry analysis as previously described [27].

Protein Identification by Mass Spectrometry

Protein digestion, nano-liquid chromatography and MS/MS mass spectrometric analysis were performed at the FingerPrints Proteomics Facility at University of Dundee, Scotland, UK. Proteins were identified by searching against the IPI protein database, and data analysis was performed as previously described [27]. Briefly, proteins identified in LNX complexes, but not in the control samples, were ranked according to Mascot protein scores and listed using gene symbols as identifiers. A Mascot protein score of 100 was then applied as a cut-off value to limit results to proteins that have been reliably identified, and probable environmental contaminants or false positives were eliminated as previously described [27].

Characterization of Interactions by GFP Pull-Down Assays

Expression vectors encoding GFP-tagged LNX1 or LNX2 constructs were transfected into HEK 293 cells, either alone or together with constructs encoding FLAG epitope-tagged LNX-interacting protein. Cultures were harvested 24–48 h post-transfection, and GFP affinity was purification performed using 10 µl GFP-Trap_M beads according to the manufacturer's protocol (ChromoTek GmbH, Planegg-Martinsried, Germany). In some cases, the wash conditions were made more stringent by increasing the NaCl concentration in the standard wash buffer up to 500 mM. Proteins were eluted by boiling in 2× SDS sample buffer and analysed by western blotting.

Statistical Analysis

The normal distribution of behavioural data was assessed using the D'Agostino–Pearson test. Two-way repeated measures analysis of variance (rANOVA) was carried out to investigate the overall effect of genotype and age on body weight profile and rotarod, followed by Bonferroni post hoc test where appropriate. Data from all other paradigms were analysed by one-way ANOVA, followed by Bonferroni post hoc test where appropriate. Statistical analyses were performed using GraphPad Prism v.6.0 (La Jolla, CA, USA). Two-tailed Student *t* tests were performed using Microsoft Excel software. *P* values of less than 0.05 were considered significant. Unless stated otherwise, all data are presented as mean ± SEM.

Results

Generation of Lnx 1/2 Double Knockout Mice

Considering the high degree of sequence and functional similarity between LNX1 and LNX2, we decided to make *Lnx 1/2* DKO mice in order to study neuronal functions of LNX proteins in vivo. To this end, we first obtained a

mouse line in which exon3 of the Lnx1 gene has been deleted (Fig. 1a). We have previously shown that this line, which we refer to as *Lnx1*$^{exon3-/-}$, lacks expression of the neuronally expressed LNX1 p70 and p62 protein isoforms (Fig. 1c) [11]. Comprehensive phenotyping of this line, which included some basic neurological and behavioural tests, did not reveal any significant findings apart from an increased percentage of B1-like B cells in peritoneal lavage (https://www.mmrrc.org/catalog/sds.php?mmrrc_id=32436). Next, we generated a *Lnx2* conditional knockout line in which exon 2 is flanked by *loxP* sites (Fig. 1b, e). Following deletion of exon 2 through Cre-mediated recombination, homozygous *Lnx2* knockout mice (*Lnx2*$^{-/-}$) were generated. These mice displayed no obvious abnormalities, and no phenotype has been reported for a different *Lnx2* KO line that was generated and phenotyped as part of the knockout mouse project (KOMP) (http://www.mousephenotype.org/data/genes/MGI:2155959).

Lnx1$^{exon3-/-}$ mice were then crossed to *Lnx2*$^{-/-}$ animals in order to generate *Lnx1*$^{exon3-/-}$; *Lnx2*$^{-/-}$ mice (DKO mice) [28]. Genotyping was performed by PCR (Fig. 1f). Similar to *Lnx1* ^{exon3} and *Lnx2* single knockouts, *Lnx* DKO mice were born at expected Mendelian frequencies, were healthy and displayed no overt phenotype. Immunoblotting was employed to characterize LNX protein expression in the murine brain and verify the absence of LNX proteins in DKO mice (Fig. 1g, h). Due to its low level of expression, LNX1 is not detectable directly in brain lysates from E14.5, P1 or P18 mice (Fig. 1g). However, immunoprecipitation of P18 brain lysates and subsequent immunoblotting using antibodies raised against LNX1 reveal the presence of the LNX1p70 and p62 isoforms in WT but not DKO P18 brain lysates. These antibodies cross react with LNX2, which is weakly detected in WT but not DKO immunoprecipitates. No compensatory upregulation of the non-neuronal LNX1p80 isoform, which would run just above LNX2, was observed in DKO animals. Using a LNX2-specific antibody, LNX2 can be detected directly in brain lysates from WT, but not DKO, E14.5, P1 and P7 mice (Fig. 1h). By contrast, LNX2 expression is barely detectable or undetectable in P18 or adult whole brain lysates. This downregulation of LNX2 protein in the early postnatal period is also apparent in immunoprecipitates from P1 and P18 animals, with LNX2 detected at P18 but at a much lower level than P1. The embryonic/early postnatal expression of LNX2 protein seems to be widespread within the CNS, with LNX2 detected in multiple brain regions, as well as the spinal cord of WT but not DKO P1 animals (Fig. 1h; lower panel). This analysis provides new information regarding LNX protein expression patterns and also validates the DKO mice as a suitable model to study the function of LNX proteins in the CNS.

Normal Gross Neuroanatomy in Lnx DKO Mice

To assess whether *Lnx1/Lnx2* deletion affects gross brain structure, we compared brain morphology in DAPI-stained sagittal sections from WT and DKO mice. Gross neuroanatomy was indistinguishable between genotypes (Fig. 2a). All major brain structures are present in DKO mice, and the cross-sectional area of major brain regions is not significantly different from WT animals (Fig. 2b). No significant differences in ventricular size were noted, and DKO brains exhibited normal lamination of neocortical and hippocampal regions. Since *Lnx1* and *2* mRNAs are prominently expressed in the cerebellum, we examined the areas of the cerebellar molecular and granule cell layers as well as the white matter and cerebellar nuclei (Fig. 2c). Again, no significant difference between genotypes was observed. These observations suggest that gross brain development proceeds normally in *Lnx* DKO mice.

Fig. 2

Gross neuroanatomy of *Lnx* DKO mice is normal. **a** DAPI staining of medial (*left*) and lateral (*right*) sagittal sections from WT and *Lnx* DKO mice. **b** Measurements of the area of major brain regions from equivalent medial sagittal sections expressed as a percentage of total slice area. $n = 4$. **c** Measurements of the area of subregions of the cerebellum (molecular layer, granule cell layer, white matter and cerebellar nuclei) expressed as a percentage of total cerebellar area. $n = 4$

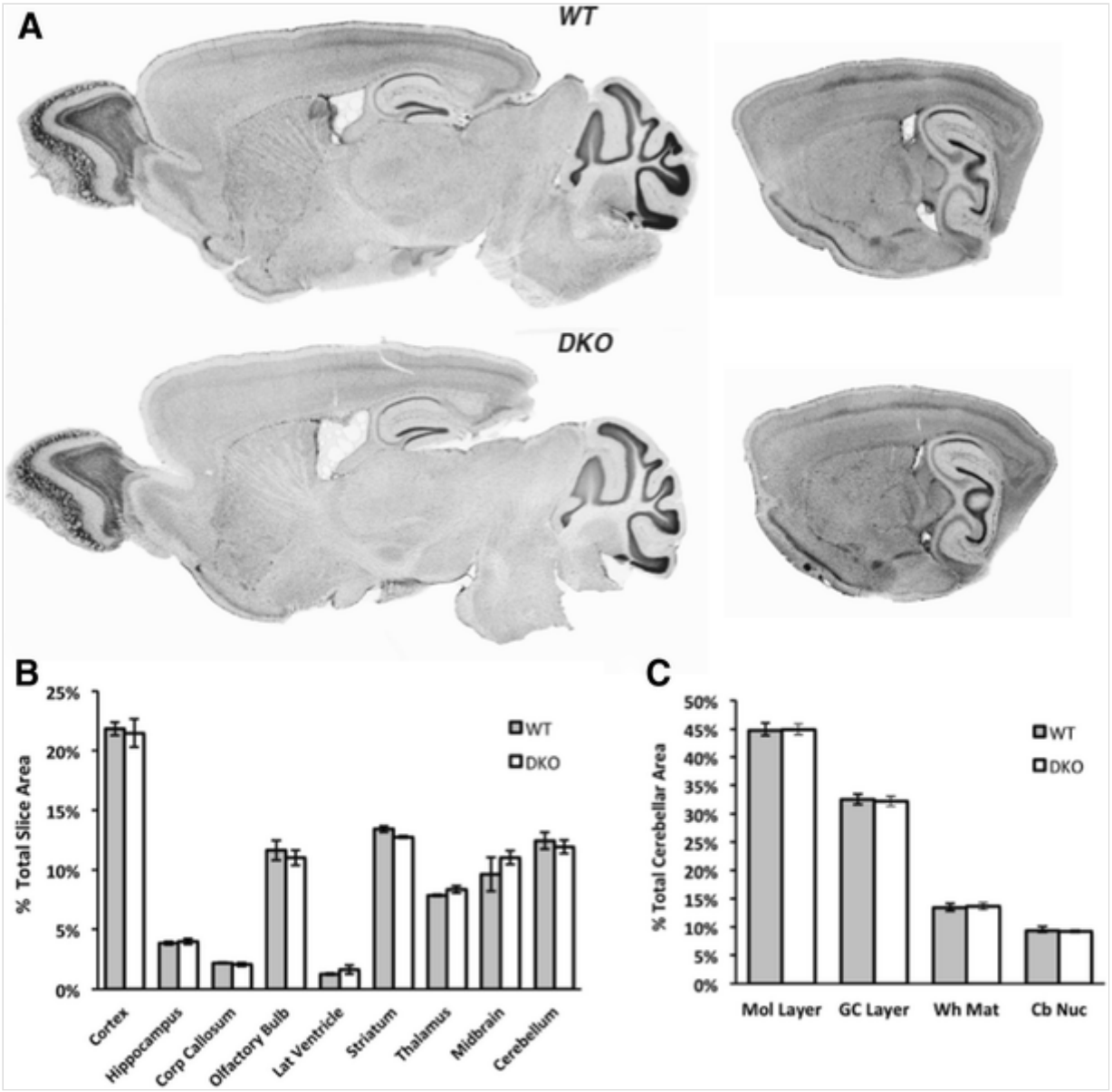

Unaltered NUMB Levels and Subventricular Zone Development Lnx DKO Mice

LNX1-mediated ubiquitination targets NUMB for proteasomal degradation [4]. LNX2 can also ubiquitinate NUMB, and it was recently proposed that LNX2 upregulation may cause the dramatic decrease in NUMB protein levels observed in *Gli3*$^{-/-}$ mice, thereby contributing to abnormalities in the development of the SVZ in these animals [5, 10]. To examine whether LNX proteins regulate NUMB levels under normal circumstances, we detected NUMB by western blotting of forebrain lysates from P1 WT and *Lnx* DKO mice—a developmental stage at which we observed relatively strong LNX2 protein expression. Three bands, which we interpret as representing three of the four known NUMB isoforms, were quantified individually (Fig. 3a). No significant differences in the levels of any NUMB isoforms were observed (Fig. 3b). Quantification of total NUMB protein at E14.5 and P18 also failed to reveal any significant alteration in NUMB levels (data not shown).

Fig. 3

Unaltered NUMB levels and normal subventricular zone (SVZ) development in *Lnx* DKO mice. **a** Protein levels of NUMB isoforms in brain lysates prepared from P1 WT and DKO mice were analysed by western blot. Blotting for vinculin verified equal protein loading in each lane. **b** Quantification of the levels of individual NUMB isoforms. No significant changes in NUMB protein levels in DKO mice were detected for any isoform, as assessed by Student's *t* test. $n = 4$. **c** *Low-magnification view* of the SVZ of P8 WT and DKO mice stained for the ependymal cell marker FOXJ1. *Scale bar* = 100 μm. **d** Co-staining of P8 WT and DKO SVZ for FOXJ1, DAPI and GFAP. *Arrowheads* indicate examples of $FOXJ1^+/GFAP^+$ double-labelled cells. *Scale bar* = μm. **e** Quantification of the proportion of $FOXJ1^+$ ependymal cells that are also $GFAP^+$. There are no significant differences between WT and DKO mice as assessed by Student's *t* test. $n = 3$. **f** Co-staining of P4 WT and DKO SVZ for LNX2 and DAPI. Any staining observed with a LNX2-specific antibody is indistinguishable between WT and DKO mice. *Scale bar* = 20 μm

AQ3

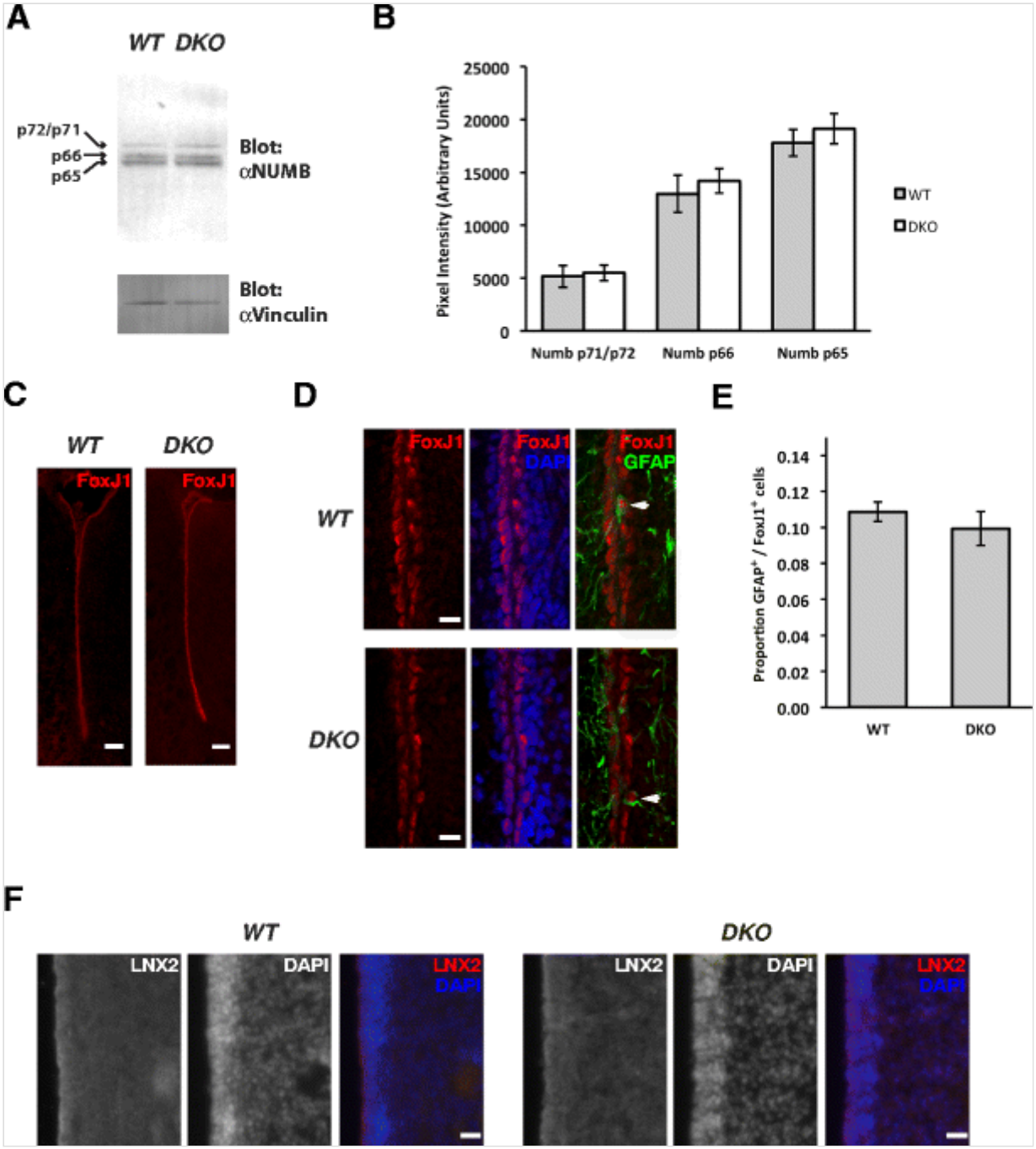

We next examined the SVZ in *Lnx* DKO mice, given that its development is abnormal in *Gli3*$^{-/-}$ mice that have elevated levels of *LNX2* protein [10]. We specifically examined the differentiation of the ependymal cells, a process that proceeds abnormally in *Gli3*$^{-/-}$ animals. Immunostaining of the SVZ at P8 for the ependymal cell marker FOXJ1 reveals normal ependymal cell maturation, with a single line of FOXJ1^{+} cells lining each ventricular wall (Fig. 3c, d). To assess cell fate specification, we co-stained for GFAP as a marker of neural stem cells and quantified the proportion of GFAP^{+}/FOXJ1^{+} double-positive cells—a parameter that is dramatically elevated in *Gli3*$^{-/-}$ mice (Fig. 3d). We observed no difference in this parameter between *Lnx* WT and DKO mice, with a low proportion of GFAP^{+}/FOXJ1^{+} cells, indicative of normal cell fate specification of ependymal cells (Fig. 3e). Finally, immunostaining of P4 SVZ of *Lnx* WT and DKO mice did not reveal a specific staining pattern for LNX2 protein that

differed between these genotypes (Fig. 3f). This staining was performed using the same antibody that detects LNX2 in forebrain lysates by western blotting. The lack of a specific staining pattern suggests that LNX2 expression in the SVZ, as in other brain regions of WT mice, is below the limit of detection by immunohistochemistry.

Behavioural Phenotyping of Lnx DKO Mice

Body Weight and Basic Sensory/Motor Function

Given the absence of gross neuroanatomical defects or obvious dysregulation of NUMB, we decided to subject *Lnx* DKO mice to a series of behavioural tests to reveal possible unanticipated physiological functions of LNX proteins in the CNS (Fig. 4a). For these analyses, both male and female WT, DHET and DKO mice were tested. Body weight was monitored weekly from 1 week of age through to the end of the testing period (Fig. 4b). For males and females, growth curves for the three genotypes started to diverge significantly at 5 and 3 weeks after birth respectively. Male DKO mice gained less weight than their WT and DHET counterparts. A similar pattern was initially observed for DKO females, though by 11 weeks female DHET mice also weighed significantly less than their WT counterparts. For males, there was a significant effect of week ($F_{12,336} = 1564$, $p < 0.0001$), genotype ($F_{2,28} = 5.098$, $p = 0.0129$) and interaction between week and genotype ($F_{24,336} = 2.653$, $p < 0.0001$) in the overall rANOVA. Similarly, for females there was also a significant effect of week ($F_{12,324} = 1351$, $p < 0.0001$), genotype ($F_{2,27} = 7.213$, $p = 0.0031$) and interaction between week and genotype ($F_{24,324} = 2.130$, $p = 0.0019$). In general, the differences in weight established during adolescence were stably maintained into adulthood and throughout the period of behavioural analysis. At 12 weeks of age, male DKO animals weighed on average 11.2 and 8.3% less than WT animals and DHET mice respectively, while female DKO and DHET mice weighed 13.2 and 10.2% less than WT mice respectively. Despite these weight differences, no mice of any genotype showed signs of ill health. Extensive primary observational testing following a modified SHIRPA protocol, as well as grip strength and hotplate tests, did not reveal significant differences between genotypes for any of 36 parameters assessed (see "Materials and Methods" section). While the weight differences between genotypes must be borne in mind, they should not preclude interpretation of other behavioural tests described below, given the absence of any other physical abnormalities or ill health in *Lnx* DKO mice.

Fig. 4

Timeline of behavioural testing and body weight analysis. **a** *Timeline* illustrating the sequence of behavioural testing and intervals between tests for both male and

female mice. **b** Effect of LNX1/LNX2 genotype on body weight gain during postnatal development. Body weights of mice were recorded weekly for the duration of the study. Initially, body weights were not different between genotypes of either sex. However, from 5 and 3 weeks of age respectively, DKO male (*left*) and female (*right*) mice weighed significantly less than their WT and DHET counterparts, and this difference in body weight persisted for the indicated period of analysis. $n = 7–12$/group. $*p < 0.05$, $**p < 0.01$, $***p < 0.001$, $****p < 0.0001$; two-way repeated measures ANOVA followed by Bonferroni post hoc test (*black* WT versus DKO, *red* DHET versus DKO, *blue* WT versus DHET)

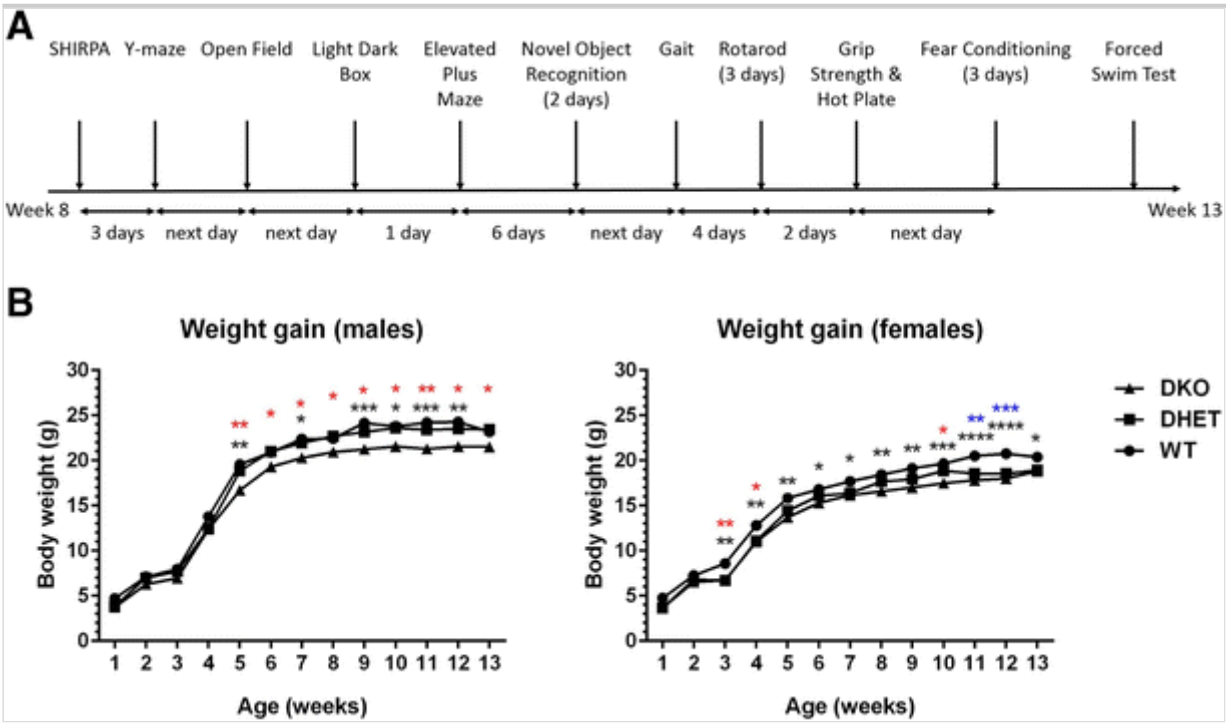

Open Field Test

The exploratory and locomotor activity of WT, DHET and DKO mice was examined by monitoring mice in an open field (Fig. 5). In male mice, no overall effect of genotype was found in total distance travelled ($F_{2,31} = 1.322$, $p = 0.2813$; Fig. 5a) or average speed of movement ($F_{2,31} = 1.255$, $p = 0.2993$; Fig. 5b). However, one-way ANOVA indicated a significant overall effect of genotype on the number of entries into ($F_{2,31} = 5.681$, $p = 0.0079$; Fig. 5c) and time spent in the centre area of the open field arena ($F_{2,31} = 8.910$, $p = 0.0009$; Fig. 5d). Bonferroni post hoc analysis revealed that DKO mice entered the centre area of the arena more frequently than their WT and DHET counterparts and spent significantly more time there ($p < 0.01$). Furthermore, one-way ANOVA indicated a significant overall effect of genotype for the time spent in the corners of the arena ($F_{2,31} = 4.694$, $p = 0.0166$; Fig. 5f). Bonferroni post hoc test revealed that DKO spent significantly less time in the corners than either

WT or DHET mice ($p < 0.05$). No difference in the number of corner entries was observed ($F_{2,31} = 0.1019$, $p = 0.9034$; Fig. 5e).

Fig. 5

Effect of *Lnx* genotype on spontaneous locomotor activity and anxiety-related behaviour in the open field task. Mice of the indicated genotypes were placed in the centre of the arena and allowed to move freely for 10 min. Distance travelled (**a**) and velocity (**b**) were analysed as indices of general locomotor activity. The number of entries into, and amount of time spent in, the centre (**c**, **d**) versus the corners (**e**, **f**) of the open field arena were monitored as indicators of differences in anxiety-like behaviour. n = 10–13/group. *$p < 0.05$, **$p < 0.01$, ***$p < 0.001$; one-way ANOVA followed by Bonferroni post hoc test

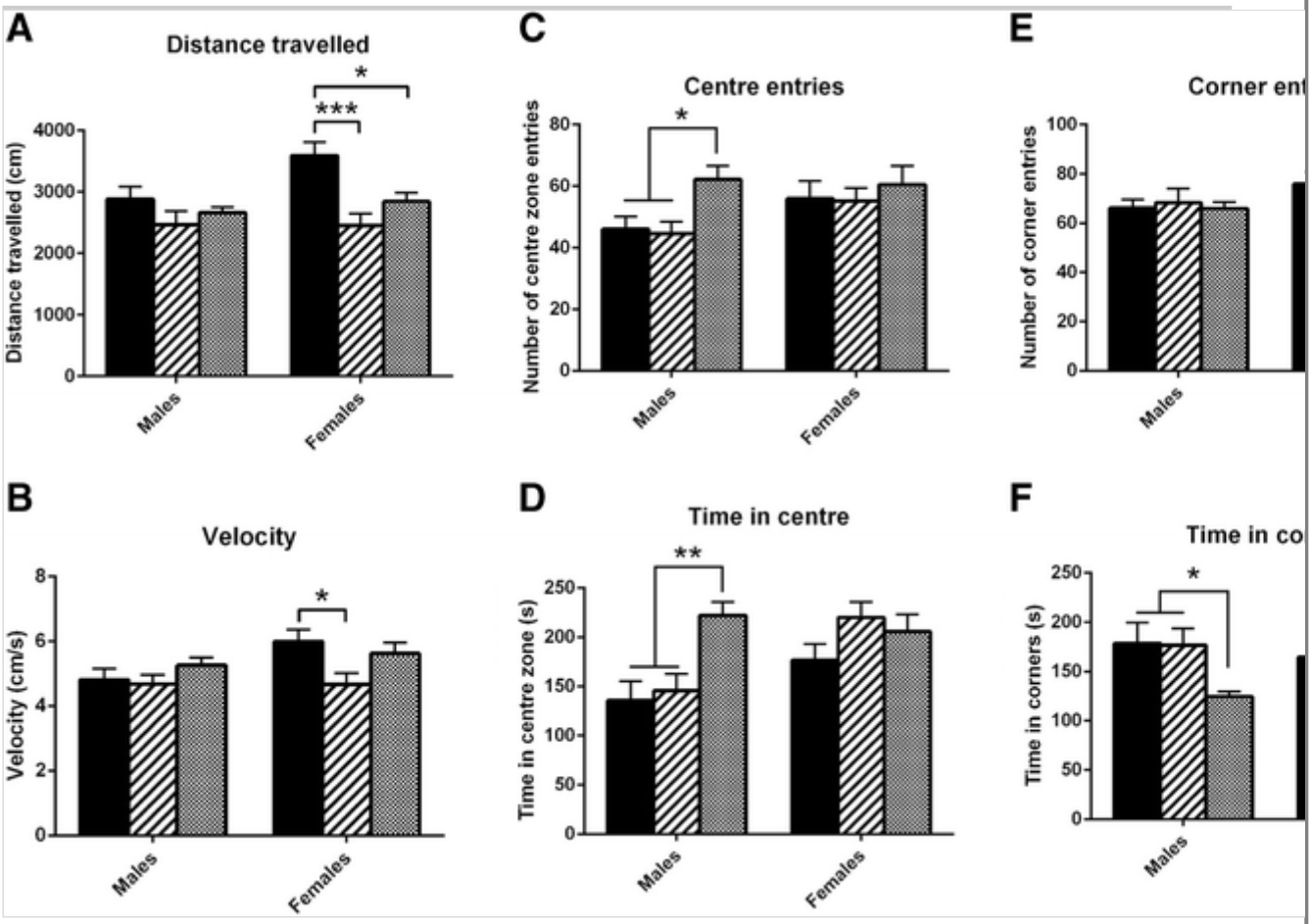

With regard to females, significant overall differences between genotypes were observed in the total distance travelled ($F_{2,31} = 9.402$, $p = 0.0006$; Fig. 5a) in the open field arena, as revealed by one-way ANOVA. Bonferroni post hoc test indicated that DHET and DKO mice travelled significantly less ($p < 0.001$ and $p < 0.05$ respectively) and, in the case of DHET, at a significantly slower average speed ($p < 0.05$) than WT controls, reflecting hypoactivity. No significant difference in the number of centre entries was detected among genotypes ($F_{2,31} = 0.2967$, $p = 0.7453$; Fig. 5c). Although DHET and DKO mice tended to spend an increased amount of time in the centre area compared to WT

controls, the effect of genotype was not significant ($F_{2,31} = 1.745$, $p = 0.1913$; Fig. 5d). A significant overall effect of genotype was detected in the number of corner entries ($F_{2,31} = 4.262$, $p = 0.0232$; Fig. 5e) and time spent in the corners of the arena ($F_{2,31} = 4.283$, $p = 0.0228$; Fig. 5f), as indicated by one-way ANOVA. Post hoc analysis revealed that DHET mice entered the corners of the arena less frequently ($p < 0.05$) and spent less time there ($p < 0.05$) than WT controls. A similar trend, though not statistically significant, was observed for DKO mice. Overall, the observation that DKO male mice spend more time in the centre and less time in the corners of the open field arena is indicative of reduced anxiety-like behaviour. Interpretation of similar trends that were seen for female DHET and DKO mice is complicated by the reduced overall locomotor activity of females of these genotypes in the open field test. Nevertheless, it is interesting to look at other tests that relate to anxiety.

Elevated Plus Maze Test

The elevated plus maze is used to analyse anxiety-related behaviour based on a preference for rodents to explore and spend time in the 'safer' environment of the closed versus the open arms of the maze [24]. For male mice, a significant effect of genotype was detected for the percentage of entries into ($F_{2,31} = 8.891$, $p = 0.0009$; Fig. 6a) and the time spent in the open arms ($F_{2,31} = 21.03$, $p \leq 0.0001$; one-way ANOVA; Fig. 6d). Bonferroni post hoc analysis revealed that DKO mice entered the open arms more frequently ($p < 0.001$ and $p < 0.05$) and spent significantly more time in the open arms ($p < 0.0001$ and $p < 0.001$) when compared to WT and DHET counterparts respectively, consistent with a phenotype characterized by a reduced anxiety-like behaviour. Conversely, significant effects of genotype on the percentage of entries into ($F_{2,31} = 8.891$, $p = 0.0009$; Fig. 6b) and the time spent in the closed arms ($F_{2,31} = 13.77$, $p = <0.0001$; Fig. 6e) were observed, with DKO mice displaying a significantly lower percentage of closed arm entries ($p < 0.001$ and $p < 0.05$) and significantly less time spent in the closed arms ($p < 0.001$) compared to WT and DHET mice respectively. One-way ANOVA indicated a significant overall effect of genotype on total number of arm entries ($F_{2,31} = 6.407$, $p = 0.0047$; Fig. 6c). Bonferroni post hoc test revealed that DHET mice exhibited a significantly lower number of total entries in comparison to WT and DKO counterparts ($p < 0.05$ and $p < 0.01$ respectively). No difference in the total number of arm entries was observed between WT and DKO mice, however, confirming that the behavioural variability between these genotypes was not as a result of differences in their locomotor activity.

Fig. 6

Effect of *Lnx* genotype on anxiety-related behaviour in the elevated plus maze. Mice of all genotypes were tested for 6 min on the elevated plus maze. **a** Percentage of entries into the open arms, **b** percentage of entries into the closed arms, **c** total arm entries, **d** time spent in the open arms and **e** time spent in the closed arms are shown. Increased entries into, and time spent in the open versus the closed arms are indicative of reduced anxiety-like behaviour. The total number of entries is an index of general locomotor activity during the task. n = 10–13/group. *$p < 0.05$, **$p < 0.01$, ***$p < 0.001$, ****$p < 0.0001$; one-way ANOVA followed by Bonferroni post hoc test

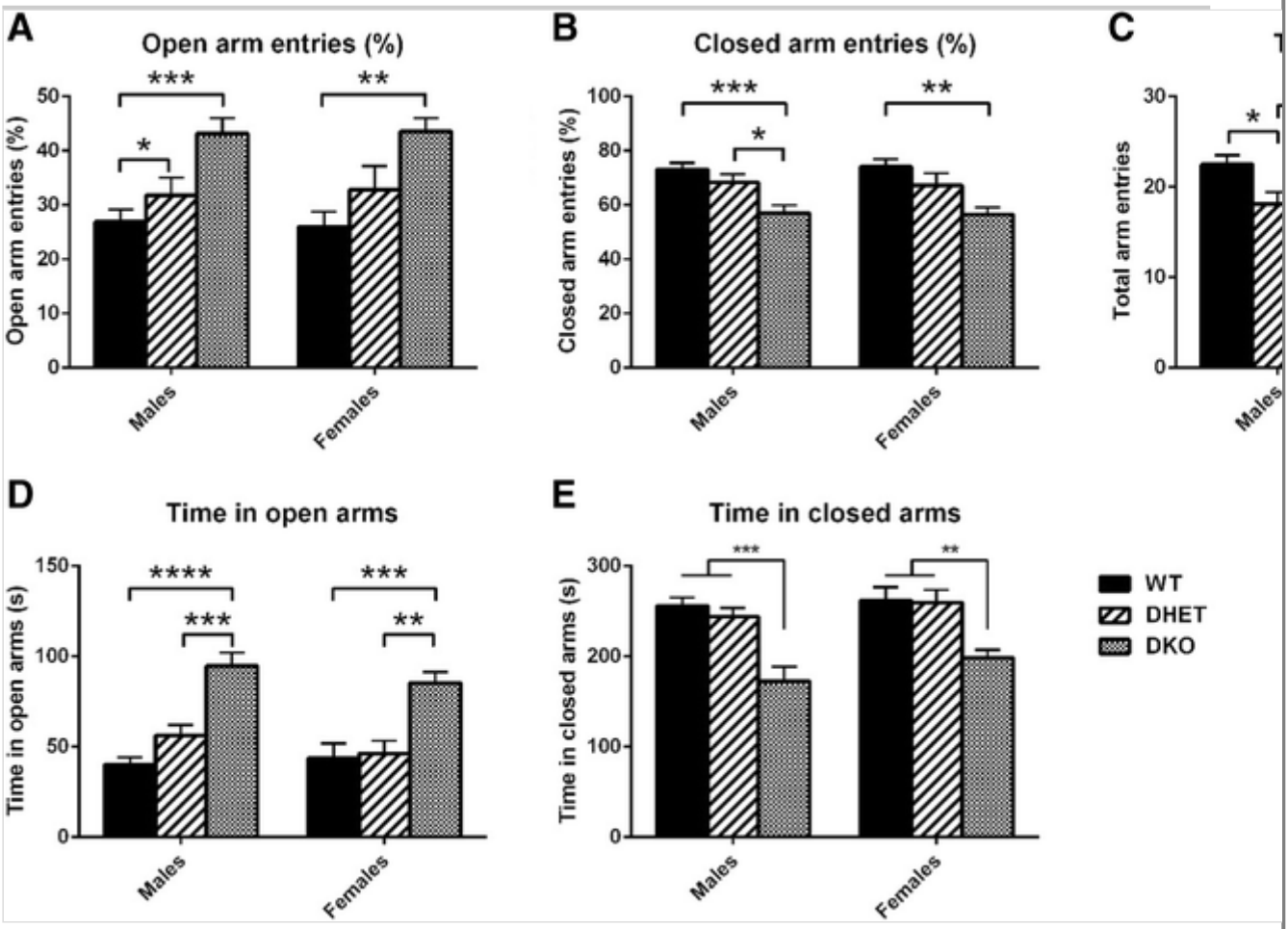

With regard to female mice, significant overall differences in the percentage of entries ($F_{2,31} = 7.362$, $p = 0.0024$; Fig. 6a) and time spent in the open arms ($F_{2,31} = 10.70$, $p = 0.0003$; Fig. 6d) of the elevated plus maze were also observed, as indicated by one-way ANOVA. Bonferroni post hoc analysis revealed that DKO mice showed a significant increase in the percentage of entries into the open arms compared to WT controls ($p < 0.01$) and an increase in the time spent in the open arms compared to WT and DHET counterparts respectively ($p < 0.001$ and $p < 0.01$). Furthermore, no differences in the total number of entries were observed ($F_{2,31} = 3.284$, $p < 0.0509$; Fig. 6c). One-way ANOVA revealed a significant effect of genotype on the percentage of entries into ($F_{2,31} = 7.362$, $p = 0.0024$; Fig. 6b) and the time spent ($F_{2,31} = 8.137$,

$p = 0.0014$; Fig. 6e) in the closed arms of the elevated plus maze. The post hoc test indicated that DKO mice entered the closed arms less often than WT mice ($p < 0.01$) and spent less time there ($p < 0.01$) than either WT or DHET mice.

Light–Dark Box Test

The light–dark box exploration paradigm, which is based on the innate aversion of rodents to brightly illuminated areas and their spontaneous exploratory behaviour, is used primarily to detect anxiogenic behaviour [24]. In this test, there were no significant overall differences between male genotypes in latency to first enter the dark compartment ($F_{2,32} = 0.07835$, $p = 0.9248$; Fig. 7a), number of light–dark transitions ($F_{2,32} = 2.501$, $p = 0.0979$; Fig. 7c) or total time spent in the light compartment ($F_{2,32} = 0.2197$, $p = 0.8040$; Fig. 7b), as revealed by one-way ANOVA. There were also no significant effects of genotype among females on latency to first enter the dark chamber ($F_{2,31} = 0.9406$, $p = 0.4012$; Fig. 7a) or total number of light–dark transitions ($F_{2,31} = 0.7211$, $p = 0.4947$; Fig. 7c). Female DKO mice did however tend to spend more time in the light compartment when compared to WT and DHET counterparts, but this difference was only marginally significant ($F_{2,31} = 3.250$, $p = 0.0533$; Fig. 7b), as revealed by one-way ANOVA.

Fig. 7

Effect of *Lnx* genotype on anxiety-related behaviour in the light/dark box. Mice were placed in the lighted compartment of the light–dark box apparatus, and latency to enter the dark compartment (**a**), time in light compartment (**b**) and the number of transitions between the light and dark compartments (**c**) were recorded for mice of the indicated genotypes and sex. Data are displayed in **a** as mean with individual data points. Analysis by one-way ANOVA did not reveal any significant effects of genotype on the parameters measured. $n = 10–13$/group

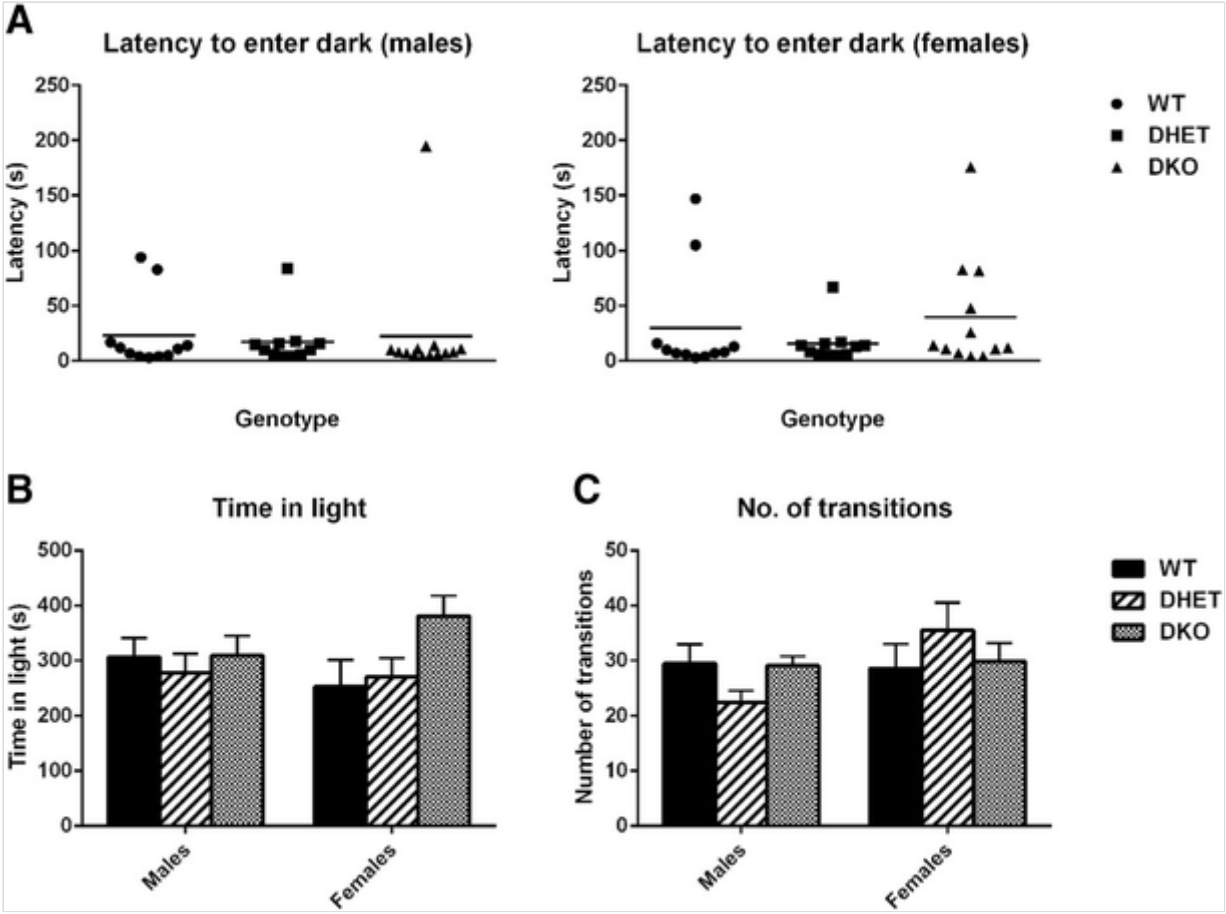

Rotarod Test

Motor coordination and skill learning were evaluated in an accelerating rotarod test. As seen in Fig. 8a, the performance of both male and female mice of all genotypes improved on the second and third days of testing, with mice remaining on the rotarod for longer durations compared to the first day of testing ($F_{2,72} = 24.74$, $p = <0.0001$ and $F_{2,58} = 9.850$, $p = 0.0002$ for males and females respectively in the overall rANOVA). Bonferroni post hoc tests revealed that the improved performance of males from day 1 to day 3 was significant for all genotypes, while those from day 1 to day 2 were significant for DKO and DHET but not WT animals ($p < 0.05$). Rotarod performance on day 1 was much better for females compared to males, and improvements across testing days was significant only for WT mice from day 1 to day 2 and DKO mice from day 1 to day 3 ($p < 0.05$). There was no overall difference between genotypes, however ($F_{2,36} = 0.9243$, $p = 0.4060$ and $F_{2,29} = 0.01303$, $p = 0.9871$ for males and females respectively), and no significant genotype by day interaction on latency to fall from the apparatus ($F_{4,72} = 0.7746$, $p = 0.5453$ and $F_{4,58} = 0.1860$, $p = 0.9448$ for males and females respectively). These observations indicate that both motor coordination and motor skill learning, as assessed by performance on the rotarod, are intact in all genotypes for both male and female mice. In agreement with this, paw print analysis did not reveal any major defects in gait (data not shown).

Fig. 8

Effect of *Lnx* genotype on learning, memory and motor coordination. **a** Analysis of motor skill learning and coordination in the accelerating rotarod test. Male (*left*) and female (*right*) mice of the indicated genotypes were placed onto an accelerating rotarod, and their latency to fall was measured in three trials per day, for three consecutive days. There were no significant differences between genotypes for either sex on any of the days as assessed by repeated measures two-way ANOVA. Improved performance on days 2 and 3 is indicative of normal motor skill learning in the task (see text). n = 9–13/group. **b** Analysis of spontaneous alternation behaviour in the Y-maze. Total entries into the arms of the maze were measured as an index of locomotor activity in the task. The number and percentage of alternations—instances where the mouse visits all three arms in sequence—were monitored as a measure of short-term spatial working memory. n = 10–13/group. *$p < 0.05$; one-way ANOVA followed by Bonferroni post hoc test

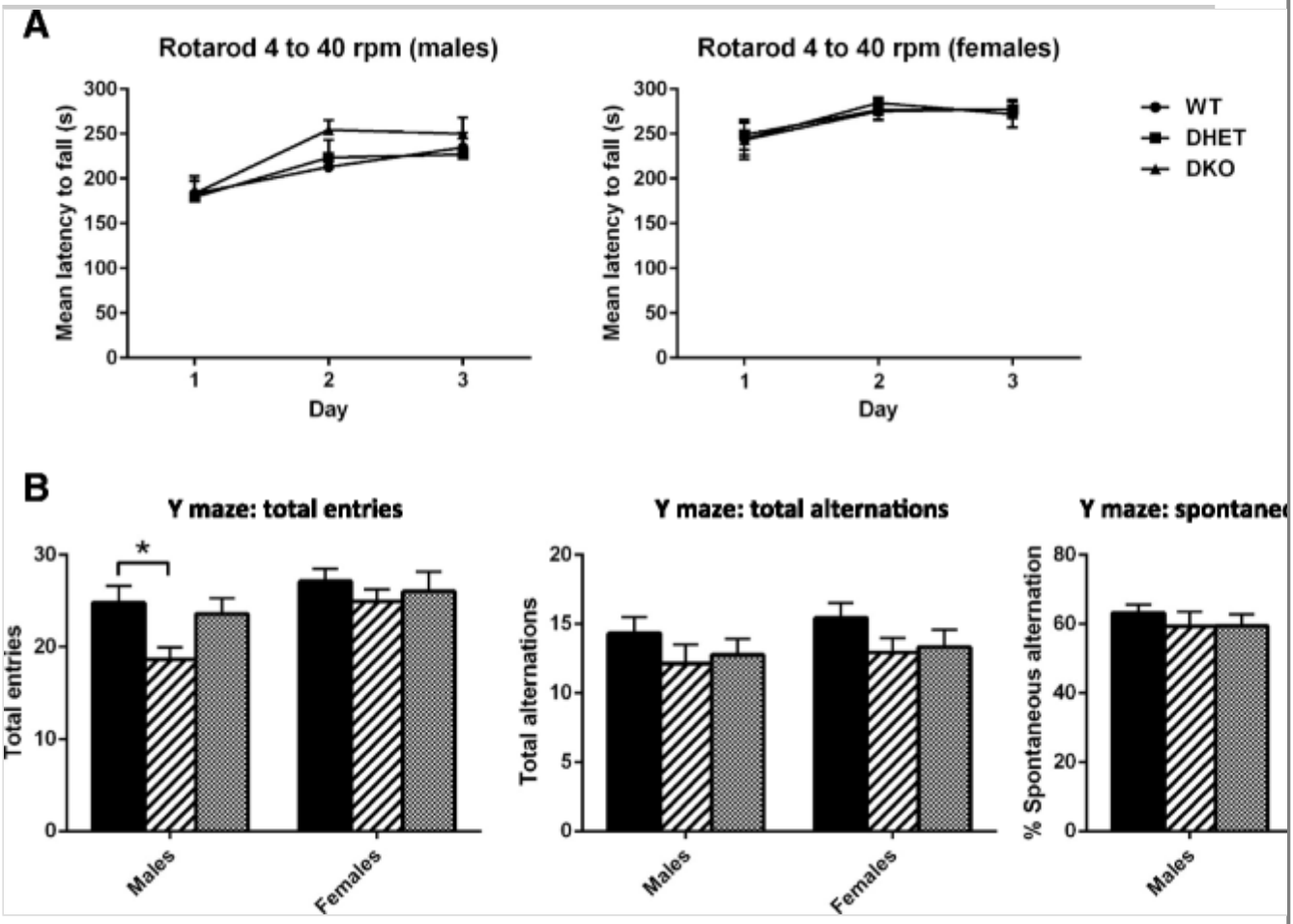

Y-Maze Test

Short-term spatial working memory was examined by monitoring spontaneous alternation behaviour in the Y-maze, a hippocampus-dependent learning task (Fig. 8b). This test relies on the inherent tendency of mice to enter a less

recently visited arm of the Y-maze. If working memory is impaired, mice will fail to remember the positions of the arms just visited and the number of alternations will be reduced [25]. Total arm entries serve as a measure of overall exploratory activity in this task. A significant overall difference between genotypes was observed in total arm entries in male mice ($F_{2,30} = 3.689$, $p = 0.0370$; Fig. 8b, left panel), with DHET mice displaying significantly less arm entries when compared to WT controls ($p < 0.05$). However, no differences in total arm entries were observed between male WT and DKO mice, indicating comparable exploratory activities between these two groups. No effect of genotype was detected in total alternations for male mice ($F_{2,30} = 0.7880$, $p = 0.4642$; Fig. 8b, middle panel). There were no overall differences between genotypes in the percentage of spontaneous alternations ($F_{2,30} = 0.4270$, $p = 0.6564$; Fig. 8b, right panel). With regard to females, there was no significant overall effect of genotype on the total number of arm entries ($F_{2,29} = 0.3615$, $p = 0.6997$; Fig. 8b, left panel), indicating comparable exploratory activity across groups. Again, no significant overall differences in total alternations ($F_{2,29} = 1.294$, $p = 0.2896$; Fig. 8b, middle panel) or in alternation percentage ($F_{2,29} = 1.559$, $p = 0.2275$; Fig. 8b, right panel) were detected. Alternation performances across genotypes were well above the random performance level of 50% for both sexes. These results indicate that there is no effect of *Lnx* genotype on spatial working memory in this task for either male or female mice.

Identification of Novel Neuronal LNX1- and LNX2-Interacting Proteins

We next sought to identify LNX-interacting proteins other than NUMB that may mediate the neuronal functions of LNX1 and LNX2, including the altered anxiety-like behaviours noted above. While many LNX-interacting proteins are known, most were found by yeast two-hybrid assays and protein/peptide arrays, and only a minority of these have been confirmed in mammalian cells using full-length proteins. Noting that a large proportion of previously reported LNX1 and LNX2 interactions involve their second PDZ domain [13, 14], we reasoned that analysis of PDZ2 may thus be sufficient to capture a significant fraction of all LNX1- and LNX2-interacting proteins. To compare the range of ligands that bind LNX1 and LNX2 PDZ2 in a neural context, we purified recombinant GST-tagged PDZ2 domains and used these proteins to ‘pull down’ interacting proteins from mouse brain lysates. Proteins identified by mass spectrometry as interacting with the PDZ domains, but not the GST tag alone, are listed in Table 1 (full lists available online in Supp. Tables 1 and 2). The known LNX-interacting proteins ERC1 and ERC2 were abundant components of both LNX1 and LNX2 complexes, as were several novel proteins such as LRRC16A,

FCHSD2, FERMT2, SHPKAP and AKAP11. LIPRIN-α proteins (PPFIA1, PPFIA3 and PPFIA4) were identified as LNX1-PDZ2-specific interacting proteins. Putative LNX2-PDZ2-specific interactions included SRGAP2, ATP2A2 and EML3.

Table 1

Proteomic analysis of LNX1 and LNX2 PDZ2 domain interactomes

Gene symbol	Mascot score	Gene name	Carboxyl terminus
A. GST-LNX1-PDZ2-interacting proteins purified from mouse brain lysates			
Erc1[a]	7959	ELKS/Rab6-interacting/CAST family member 1	DQDEEEGIWA
Ppfia3	4094	Liprin-alpha-3	DGVSVRTYSC
Erc2[a]	2235	ELKS/Rab6-interacting/CAST family member 2	DQDDEEGIWA
Lrrc16a[a]	2180	Leucine-rich repeat-containing protein 16A	EEAEKEFIFV
Fchsd2[a]	2109	FCH and double SH3 domains protein 2	KMEDVEITLV
Ppfia4	1549	Liprin-alpha-4	EPSTVRTYSC
Fermt2[a]	1467	Fermitin family homologue 2	MFYKLTSGWV
Ppfia2	1441	Liprin-alpha-2	DNSTVRTYSC
Ppfia1	1358	Liprin-alpha-1	DSATVRTYSC
Ppp2r5d	968	Protein phosphatase 2A B56 delta subunit	TGSRNGREGK
Prkcc	843	Protein kinase C gamma type	PTSPVPVPVM
Akap11[a]	792	A-kinase anchor protein 11	ANRLQTSMLV
Ndrg3	749	N-myc downstream regulated gene NDRG3	DRHQTMEVSC
Ppp2r5c	724	Serine/threonine-protein phosphatase 2A 56 kDa regulatory subunit gamma isoform	ASELLSQDGR
Pafah1b1[a]	710	Platelet-activating factor acetylhydrolase IB subunit alpha	DQTVKVWECR
B. GST-LNX2-PDZ2-interacting proteins purified from mouse brain lysates			
Erc1[a]	3181	ELKS/Rab6-interacting/CAST family member 1	DQDEEEGIWA
Sphkap[a]	2692	A-kinase anchor protein SPHKAP	EQKERTPSLF

Gene symbol	Mascot score	Gene name	Carboxyl terminus
Lrrc16a[a]	2240	Leucine-rich repeat-containing protein 16A	EEAEKEPTV
Fchsd2[a]	1938	FCH and double SH3 domains protein 2	KMEDVEITLV
Srgap2	1935	SLIT-ROBO Rho GTPase-activating protein 2	PQATDKSCTV
Akap11[a]	1576	A-kinase anchor protein 11	ANRLQTSMLV
Fermt2[a]	1287	Fermitin family homologue 2	MFYKLTSGWV
Erc2[a]	1139	ELKS/Rab6-interacting/CAST family member 2	DQDDEEGIWA
Atp2a2	1125	SERCA2B of sarcoplasmic/endoplasmic reticulum Ca^{++} ATPase2	DTNFSDMFWS
Rrbp1	1059	Rrbp1 ribosome-binding protein 1 isoform a	GSSSKEGTSV
Kazn[a]	560	Isoform 1 of Kazrin	GYGSLEVTNV
Eml3	549	Eml3 echinoderm microtubule-associated protein-like 3	SLSPASSLDV
Prkar1b[a]	507	cAMP-dependent protein kinase type I-beta regulatory subunit	RYNSFISLTV
Prkar1a[a]	504	cAMP-dependent protein kinase type I-alpha regulatory subunit	QYNSFVSLSV
Ktn1	500	Ktn1 uncharacterized protein	EVNQQLTKET

Selected proteins, ranked by Mascot score, are shown for each experiment. Full tables are available as supplementary material. Previously known interactions are underlined, as are carboxyl-terminal cysteines

[a]A protein identified as interacting with both LNX1 and LNX2 PDZ2 domains

AQ4

We next assessed the ability of a selection of these proteins to interact with full-length LNX1 and LNX2 proteins using GFP pull-down assays, employing GFP-tagged LNX proteins expressed in cultured cells (Fig. 9). LIPRIN-α proteins again bound specifically to LNX1 in this assay, while FCHSD2, SRGAP2, ERC1 and ERC2 interacted with both full-length LNX1 and LNX2. Notably, SRGAP2 was able to interact with full-length LNX1, even though it was only detected in LNX2–PDZ2 and not LNX1–PDZ2 complexes from brain lysates. By contrast, the FERMT2 interaction could not be confirmed with full-length LNX1 or LNX2 proteins. Overall, our GST pull-down analysis of LNX PDZ2 domains identified 58 putative LNX1-specific, 39 putative LNX2-specific and 26 apparently

common interactions (Supp. Tables 1 and 2). However, verification of these interactions and their specificity using full-length LNX1 and LNX2 proteins is clearly necessary.

Fig. 9

Verification of the ability of candidate interacting proteins to bind full-length LNX1 and/or LNX2. Selected proteins that co-purified with either LNX1-PDZ2 or LNX2-PDZ2 from brain lysates were tested for their ability to interact with full-length, GFP-tagged LNX1 and/or LNX2 constructs following co-transfection into ssHEK293 cells. Following a GFP 'pull-down' assay, LNX-interacting proteins were detected by western blotting via either a FLAG epitope tag or using an antibody to detect endogenous protein in the case of LIPRIN-α3. GFP alone was used as a negative control (not visible on blots due to its low molecular weight)

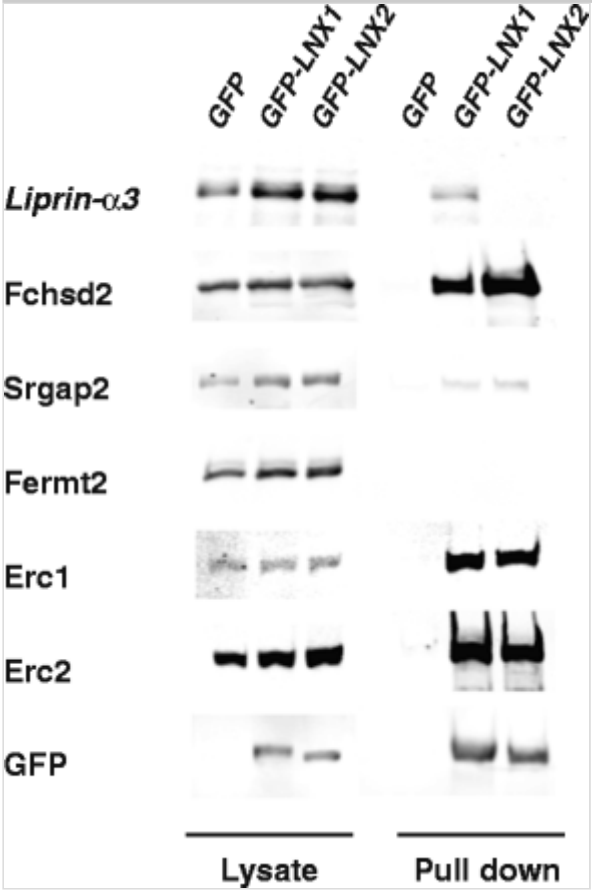

Discussion

The function of LNX proteins in vivo remains unknown, largely because LNX proteins are present at exceedingly low levels in most adult tissues. *Lnx1* and *Lnx2* mRNAs are expressed prominently in the CNS during embryonic development, with strong *Lnx2* mRNA expression in the forebrain being particularly noteworthy [2]. Here, we show that both LNX1 and LNX2 proteins are present in the juvenile murine brain, albeit at low levels. LNX2 protein is detectable at embryonic and early postnatal stages, but decreases dramatically

thereafter. Given that *Lnx2* mRNA expression persists into adulthood, the downregulation of LNX2 expression seems to be occurring post-transcriptionally, possibly at the level of translation as has been described for LNX1 [2, 11], although a high protein turnover rate may also contribute to the low levels of LNX proteins observed in vivo.

Since LNX proteins interact with and can ubiquitinate and promote the proteasomal degradation of the key cell fate-determinant protein NUMB [2, 3, 4, 5], we hypothesized that they may play a role in regulating neuronal development or function in some way. Here, we sought to test this hypothesis by generating *Lnx DKO* mice, in which expression of all CNS LNX protein isoforms is eliminated. In these mice, LNX2 is expected to be eliminated globally in all tissues, while the loss of LNX1 is expected to be restricted to the exon 3-containing, CNS-specific LNX1 p70 and p62 isoforms. In agreement with this, we previously noted intact immunostaining for what is presumed to be the LNX1 p80 isoform in perisynaptic Schwann cells in the PNS of these $Lnx1^{exon3-/-}$ mice [11, 17]. *Lnx* DKO mice are viable and fertile and display no overt phenotype, apart from weighing approximately 10% less than WT animals by adulthood. This weight difference only became noticeable at, or soon after, weaning age and could be a consequence of some function of LNX2 outside the CNS. Tooth development appeared to be normal, and DKO animals showed no difficulty eating, so perhaps a role for LNX2 in the gut or in regulating some aspect of metabolism could be responsible. However, DKO mice seem completely healthy despite their slightly lower body weight and thus represent a valid model to examine neuronal functions of LNX proteins.

NUMB and NUMBLIKE regulate multiple aspects of neural development, from early embryonic through postnatal stages. During early mouse cortical neurogenesis, asymmetric localization of NUMB in dividing ventricular cells promotes an undifferentiated progenitor cell fate [29, 30], but at later developmental stages or in other cellular contexts, NUMB has been shown to promote neuronal differentiation [31, 32, 33]. While NUMB and NUMBLIKE have a well-established role as negative regulators of Notch signalling, some aspects of their neuronal functions are thought to be Notch-independent, mediated via regulation of hedgehog signalling and cadherin-based cell adhesion [7]. NUMB knockout in mice causes a failure of neural tube closure and is lethal by E11.5, while NUMB/NUMBLIKE double knockout embryos are more severely affected and die by E9.5 [29, 33, 34]. Various studies employing conditional knockout of NUMB, often in a NUMBLIKE null background, have highlighted essential roles for NUMB/NUMBLIKE in regulating neural progenitor cell maintenance, cortical development, organization and lamination, ventricular size, cerebellar granule cell maturation and migration and SVZ

formation [9, 29, 31, 35, 36, 37]. *Lnx2* mRNA is expressed as early as E11.5 in the neuroepithelium [2], and we have shown here that LNX2 protein is expressed in the brain from E14.5 to P7. A role for LNX2 in negatively regulating NUMB levels during the later stages of cortical neurogenesis thus seems plausible. However, we do not observe any defects in gross neuroanatomy in DKO mice and cortical organization and lamination appear normal. Similarly, we did not note any malformation of cell layers in the cerebellum, another region with strong *Lnx1* and *Lnx2* mRNA expression and one where NUMB has been shown to regulate granule cell maturation and migration [2, 31].

We also examined the development of the neurogenic SVZ—an early postnatal NUMB-dependent process [9]. Conditional NUMB/NUMBLIKE knockout mice show severe damage to and enlargement of the lateral ventricles, and a recent report has implicated LNX2 in regulating NUMB levels in the SVZ in the context of *Gli3* knockout mice [9, 10]. The Gli3 transcriptional repressor is a sonic hedgehog signalling component that was shown to be required for cell-type specification and structural organization in the developing SVZ, phenocopying to a degree, NUMB loss-of-function mutants. Indeed, $Gli3^{-/-}$ mice were reported to have dramatically reduced forebrain NUMB protein levels [10]. This finding was attributed to upregulation of LNX2 in the SVZ of these mice; however, a causal relationship between LNX2 and NUMB levels in $Gli3^{-/-}$ mice remains to be established. In any case, our data suggest that SVZ zone formation and ependymal cell differentiation proceed normally in *Lnx* DKO mice and that LNX2 at normal expression levels is not affecting NUMB function in SVZ formation. These findings are in agreement with the observation of unaltered levels of any NUMB protein isoforms in *Lnx* DKO mice. It has been found that while LNX1 is able to interact with all four NUMB isoforms, only those containing a short sequence insertion in the PTB domain (p66 and p72) are ubiquitinated by LNX1 [3]. Thus, we would not necessarily expect LNX to regulate levels of NUMB p65 or p71, assuming that the same specificity with regard to NUMB ubiquitination applies to LNX2. However, even the levels of NUMB p66, which should be prone to LNX-mediated ubiquitination, are unaltered in DKO mice. This suggests that endogenous LNX2 expression levels are not sufficient to promote ubiquitin-mediated degradation of NUMB or that LNX2 and NUMB are not widely co-expressed in the same cells in vivo. We cannot rule out however that some LNX-mediated degradation of NUMB may occur in a temporally or spatially restricted manner. Unfortunately, we could not detect LNX2 by immunostaining to address this issue. Overall though, our analysis of *Lnx* DKO animals does not provide any direct evidence that LNX proteins are major regulators of NUMB in vivo, since no obvious defects in NUMB-dependent processes are observed.

Given this lack of evidence for NUMB dysregulation, we proceeded to conduct behavioural phenotyping of *Lnx* DKO mice. Since there are few clues in the literature regarding neuronal functions of LNX proteins in vivo, we performed a battery of tests to screen for a broad range of potential phenotypes. The main phenotype identified was one of reduced anxiety-like behaviour. This was assessed in three approach-avoidance paradigms: the open field test, the light–dark box test and the elevated plus maze. These tests are based on the conflict between the innate exploratory behaviour of rodents and their aversion towards open, bright or elevated spaces, which carry an associated risk of predation [24]. The anxiolytic phenotype was very robust in the elevated plus maze, with DKO mice of both sexes exhibiting increased entries into, and time spent in, the open arms of the maze. Male DKO animals also spent more time exploring the centre versus the corners of the arena in the open field test. A similar trend was observed for females in the open field, but this data was confounded by the fact that DHET and DKO females showed less overall locomotor activity in this task. By contrast, no effect of *Lnx* genotype was seen for either sex in latency to enter the dark compartment, the number of transitions between light and dark sides or time spent in the light compartment in the light–dark box test. While obtaining consistent findings across multiple tests is generally strong evidence for a particular phenotype, it is recognized that various tests of anxiety in rodents do not measure exactly the same psychological phenomenon. Rather, each test can be regarded as measuring overlapping, but partially distinct, aspects of anxiety-related behaviour [24]. Thus, knockout models with both anxiogenic and anxiolytic phenotypes that are specific to particular tests have previously been reported [21, 38]. Overall, reports on transgenic and knockout mice with reduced anxiety-like behaviour are not uncommon in the literature, though anxiolytic indications are sometimes found in combination with other behavioural deficits [39]. *Lnx* DKO mice did not show any deficiencies in basic motor function, or in motor coordination or motor skill learning as assessed by the rotarod test, despite the fact that *Lnx1* and *Lnx2* mRNAs are expressed in the motor cortex, spinal cord and cerebellum [2, 11] and the observation that Numb can influence these behaviours [40]. Sensory function and spatial working memory, as measured by spontaneous alternation in the Y-maze, were also unaffected. Thus, the reduced anxiety-like behaviour observed for DKO mice seems to be a very specific phenotype that is restricted to a subset of anxiety-related testing paradigms.

The anxiolytic phenotype reported here for *Lnx* DKO mice clearly merits further investigation. Genetic analyses will determine if either *Lnx1* or *Lnx2* single knockout animals display the same phenotype or whether the simultaneous loss of both genes is responsible. The use of conditional approaches to spatially

restrict knockout of one or both genes should allow the brain region(s) responsible for the phenotype to be identified. Temporally restricted *Lnx* knockout could address the question of whether the phenotype arises from a developmental defect or from the absence of LNX proteins from the adult brain at the time of behavioural testing. It will also be interesting to subject *Lnx* DKO mice to a wider array of behavioural tests that may be able, for example, to dissociate decreased anxiety-related behaviour from any increased novelty seeking or impulsivity that could contribute to increased time spent in novel, aversive areas in the open field and elevated plus maze paradigms [24]. More extensive testing may also reveal phenotypes beyond the decreased anxiety-related behaviour described here. Finally, examining the effects of known anxiogenic or anxiolytic pharmacological agents in *Lnx* DKO mice might identify neurotransmitter systems or signalling pathways responsible for the reduced anxiety-like phenotype. Studies of the type outlined above should determine whether LNX protein could represent a novel drug target, whereby selective blockade of LNX function or expression would have therapeutic potential in anxiety disorders.

It is important to elucidate the neurobiological circuits and pathways that are altered by ablation of *Lnx1* and *Lnx2* in DKO mice, generating the anxiolytic-like phenotype. Although we found no change in NUMB levels in DKO mice, we cannot rule out that this phenotype may be attributed to the interaction of LNX proteins with NUMB. For example, LNX could regulate NUMB by mechanisms other than promoting its proteasomal degradation, such as altering its subcellular localization. Indeed, the absence of the RING domain from neuronal LNX1 isoforms suggests ubiquitination-independent functions [1, 11]. Nevertheless, given the absence of obvious NUMB-related abnormalities in DKO mice, the possibility that LNX functions in the CNS are mediated by interacting proteins other than NUMB needs to be considered. Many LNX1-interacting proteins have been identified [13, 14]. Most of these are PDZ domain ligands, with the second PDZ domain mediating a large proportion of these interactions. However, the physiological relevance of the vast majority of these reported interactions is unclear. Fewer LNX2-interacting proteins have been reported, and the LNX1 and LNX2 interactomes have never been systematically compared. To address these issues, we used an affinity purification/mass spectrometry-based approach to isolate and identify proteins from P16 mouse brain lysates that bind the second PDZ domain of each protein. Five out of six interactions tested could be confirmed with full-length LNX proteins, validating the approach of using a single PDZ domain as a bait to isolate meaningful interactions.

These proteomic results provide confirmation of just four of the approximately 250 previously reported LNX interactions (BCR, CTNND2, ERC2, KRT15) [13, 14]. This partly reflects our focus on just the second PDZ domain and the fact that previously reported proteins may not be expressed in P16 mouse brain tissue. However, it may be that some interaction pairs that have been identified by yeast two-hybrid or protein/peptide arrays are not significant in a physiological context, in which many potential ligands can bind competitively to LNX proteins. Many of the proteins we identified have carboxyl terminal sequences that fit consensus sequences previously identified for LNX1 and LNX2 PDZ2 [14], suggesting that they interact with LNX proteins directly. The identification of putative LNX1 PDZ2-interacting proteins with carboxyl terminal cysteines is particularly noteworthy, with ten such proteins found in LNX1 complexes as compared to just one for LNX2 PDZ2. Notable LNX1-specific interactors with carboxyl terminal cysteines are members of the LIPRIN-α (PPFIA1, PPFIA2, PPFIA3, PPFIA4) and N-myc downstream-regulated gene (NDRG1, NDRG2, NDRG3) families. The LNX1-specific interaction of LIPRIN-α3 was confirmed in assays using full-length LNX proteins. In addition, some indirect interactions are likely to have been detected by our affinity purification approach, which may partly explain the lack of overlap with LNX ligands previously identified using methods that favoured detection of direct interactions. For example, the protein phosphatase 2A regulatory subunits (PPP2R5C and PPP2R5D) lack a carboxyl terminal PDZ-binding consensus sequence but are known to interact with LIPRIN-αs [41, 42]. This suggests that their specific co-purification with LNX1 PDZ2 may be due to an indirect interaction mediated by LIPRIN-α. In any case, such isoform-specific interactions, whether direct or indirect, provide clues regarding differential functions of LNX1 and LNX2—an area that has not previously been explored.

Comparing the lists of 84 LNX1- and 65 LNX2-interacting proteins (Supp. Tables 1 and 2), there is considerable overlap (26 proteins). Notable interactions common to PDZ2 of both LNX1 and LNX2 are the ELKS/Rab6-interacting/CAST family members ERC1 and ERC2. LNX1 is known to interact with ERC2 [43]. Our data confirm this and indicate that this ability is shared by LNX2. Interestingly, ERC and liprin-α proteins interact with each other and are evolutionarily conserved core components of the presynaptic active zone complex that underpins synapse formation and maturation, as well as neurotransmitter release [44, 45]. ERC1/2 and liprin-αs are likely to bind competitively to LNX1–PDZ2; however, LNX1 is known to dimerise [2], and so a LNX1 dimer could potentially form a tripartite complex binding both ERC and liprin-α proteins simultaneously. Higa et al. [43] reported that LNX1 and ERC2 co-localize at nerve terminals in cultured neurons. Our findings that

LNX2 also binds ERC1/2 and that LNX1 binds liprin-α now provide further support for a potential function for LNX proteins at the active zone. While probably not abundant enough to play a structural role, they might regulate some aspect of active zone formation or plasticity. Kazrin (KAZN) was another interaction shared by LNX1 and LNX2 and interestingly has been described as belonging to the LIPRIN protein family [46]. The SLIT-ROBO Rho GTPase-activating proteins, SRGAP1 and SRGAP2, were co-purified with LNX1 and LNX2 PDZ2 domains respectively. However, in confirmatory assays using full-length LNX proteins, SRGAP2 bound both LNX1 and LNX2 and so was not isoform-specific in its interaction. SRGAP2 acts as a regulator of neuronal migration, neurite outgrowth and dendritic spine formation and plays important roles in cortical development, with human-specific duplications of SRGAP2 hypothesized to have played a role in the evolution of the human neocortex [47, 48, 49, 50]. FCHSD2, which we identified as binding to both LNX1 and LNX2 via PDZ2, is evolutionarily related to the SRGAP proteins, having in common the presence of an F-BAR and SH3 domains in its domain structure, but lacking the GTPase-activating domain. FCHSD2 is a mammalian homologue of *nervous wreck* (*nwk*)—a regulator of synaptic growth in *Drosophila* [51]. Other putative LNX1- and LNX2-interacting proteins identified include regulatory subunits of protein kinase A (PRKAR1A and PRKAR1B) and a GABA neurotransmitter transporter (SLC6A1). Overall, this analysis confirms the propensity of LNX proteins to interact with a large number of ligands via their PDZ domains and provides a catalogue of putative interacting partners that will be a valuable resource in exploring the molecular mechanism of LNX function in the CNS. Subject to further validation, this brain-specific interactome identifies many plausible candidates that could mediate neuronal functions of LNX proteins in the CNS, including their role in modulating anxiety-related behaviour.

In summary, this is the first study of the in vivo functions of LNX1 and LNX2 in a mammalian context. Zebrafish have an additional LNX paralogue—LNX2b—which has been studied extensively and found to modulate transcription factors involved in dorso-ventral and antero-posterior axis specification during embryogenesis [52, 53, 54]. The relatively mild phenotype of *Lnx* DKO mice suggests that mammalian LNX proteins do not have analogous functions to fish LNX2b. While our findings do not provide evidence of a major role for LNX in regulating NUMB during mammalian CNS development, we cannot exclude a subtle role. An unexpected function for LNX proteins in the regulation of anxiety-related behaviour has been revealed. However, the molecular mechanisms and the brain regions underlying this behavioural phenotype need further investigation in order to gain a more complete understanding of LNX protein function in vivo.

Acknowledgements

We are extremely grateful to Pat Fitzgerald and James O'Leary for their generous assistance and advice regarding behavioural experiments. We thank Mary McCaffrey (University College Cork) for access to her Science Foundation Ireland-funded confocal microscope and Jane McGlade (University of Toronto) for providing the rabbit anti-LNX1/2-RING/NPAY antibody. This work was supported by a Research Frontiers Programme grant from Science Foundation Ireland (08/RFP/NSC1382) and an Irish Research Council EMBARK Postgraduate Research Scholarship to Joan Lenihan.

Compliance with Ethical Standards

All animal experiments were approved by the Animal Experimentation Ethics Committee of University College Cork (No: 2013/028) and were conducted under licence (No: AE19130/P013) issued by the Health Products Regulatory Authority of Ireland, in accordance with the European Union Directive 2010/63/EU for animals used for scientific purposes.

Conflict of Interest The authors declare that they have no conflict of interest.

Electronic supplementary material

ESM 1

(PDF 155 kb)

References

1. Dho SE, Jacob S, Wolting CD, French MB, Rohrschneider LR, McGlade CJ (1998) The mammalian numb phosphotyrosine-binding domain. Characterization of binding specificity and identification of a novel PDZ domain-containing numb binding protein, LNX. J Biol Chem 273:9179–9187

2. Rice DS, Northcutt GM, Kurschner C (2001) The Lnx family proteins function as molecular scaffolds for Numb family proteins. Mol Cell Neurosci 18:525–540

3. Nie J, Li SS, McGlade CJ (2004) A novel PTB-PDZ domain interaction mediates isoform-specific ubiquitylation of mammalian Numb. J Biol Chem 279:20807–20815

4. Nie J, McGill MA, Dermer M, Dho SE, Wolting CD, McGlade CJ (2002) LNX functions as a RING type E3 ubiquitin ligase that targets the cell fate determinant Numb for ubiquitin-dependent degradation. EMBO J 21:93–102

5. Nayak D, Sivaraman J (2015) Structural basis for the indispensable role of a unique zinc finger motif in LNX2 ubiquitination. Oncotarget 6:34342–34357

6. Camps J et al. (2013) Genetic amplification of the NOTCH modulator LNX2 upregulates the WNT/beta-catenin pathway in colorectal cancer. Cancer Res

7. Gulino A, Di Marcotullio L, Screpanti I (2010) The multiple functions of Numb. Exp Cell Res 316:900–906

8. Weiss A, Baumgartner M, Radziwill G, Dennler J, Moelling K (2007) C-Src is a PDZ interaction partner and substrate of the E3 ubiquitin ligase ligand-of-Numb protein X1. FEBS Lett 581:5131–5136

9. Kuo CT et al (2006) Postnatal deletion of Numb/Numblike reveals repair and remodeling capacity in the subventricular neurogenic niche. Cell 127:1253–1264

10. Wang H, Kane AW, Lee C, Ahn S (2014) Gli3 repressor controls cell fates and cell adhesion for proper establishment of neurogenic niche. Cell Rep 8:1093–1104

11. Lenihan JA, Saha O, Mansfield LM, Young PW (2014) Tight, cell type-specific control of LNX expression in the nervous system, at the level of transcription, translation and protein stability. Gene 552:39–50

12. Flynn M, Saha O, Young P (2011) Molecular evolution of the LNX gene family. BMC Evol Biol 11:235

13. Wolting CD, Griffiths EK, Sarao R, Prevost BC, Wybenga-Groot LE, McGlade CJ (2011) Biochemical and computational analysis of LNX1 interacting proteins. PLoS One 6:e26248

14. Guo Z et al (2012) Proteomics strategy to identify substrates of LNX, a PDZ domain-containing E3 ubiquitin ligase. J Proteome Res 11:4847–4862

15. D'Agostino M, Tornillo G, Caporaso MG, Barone MV, Ghigo E, Bonatti S, Mottola G (2011) Ligand of Numb proteins LNX1p80 and LNX2 interact with the human glycoprotein CD8alpha and promote its ubiquitylation and endocytosis. J Cell Sci 124:3545–3556

16. Takahashi S, Iwamoto N, Sasaki H, Ohashi M, Oda Y, Tsukita S, Furuse M (2009) The E3 ubiquitin ligase LNX1p80 promotes the removal of claudins from tight junctions in MDCK cells. J Cell Sci 122:985–994

17. Young P, Nie J, Wang X, McGlade CJ, Rich MM, Feng G (2005) LNX1 is a perisynaptic Schwann cell specific E3 ubiquitin ligase that interacts with ErbB2. Mol Cell Neurosci 30:238–248

18. Heyer MP, Pani AK, Smeyne RJ, Kenny PJ, Feng G (2012) Normal midbrain dopaminergic neuron development and function in miR-133b mutant mice. J Neurosci 32:10887–10894

19. Heimer-McGinn V, Young P (2011) Efficient inducible Pan-neuronal cre-mediated recombination in SLICK-H transgenic mice. Genesis 49:942–949

20. Schneider CA, Rasband WS, Eliceiri KW (2012) NIH image to ImageJ: 25 years of image analysis. Nat Methods 9:671–675

21. Crawley JN (2008) Behavioral phenotyping strategies for mutant mice. Neuron 57:809–818

22. Irwin S (1968) Comprehensive observational assessment: Ia. A systematic, quantitative procedure for assessing the behavioral and physiologic state of the mouse. Psychopharmacologia 13:222–257

23. Rogers DC, Fisher EM, Brown SD, Peters J, Hunter AJ, Martin JE (1997) Behavioral and functional analysis of mouse phenotype: SHIRPA, a proposed protocol for comprehensive phenotype assessment. Mamm Genome 8:711–713

24. Cryan JF, Holmes A (2005) The ascent of mouse: advances in modelling human depression and anxiety. Nat Rev Drug Discov 4:775–790

25. Hughes RN (2004) The value of spontaneous alternation behavior (SAB) as a test of retention in pharmacological investigations of memory. Neurosci Biobehav Rev 28:497–505

26. Murphy AC, Lindsay AJ, McCaffrey MW, Djinovic-Carugo K, Young PW (2016) Congenital macrothrombocytopenia-linked mutations in the actin-binding domain of alpha-actinin-1 enhance F-actin association. FEBS Lett 590:685–695

27. Foley KS, Young PW (2013) An analysis of splicing, actin-binding properties, heterodimerization and molecular interactions of the non-muscle alpha-actinins. Biochem J 452:477–488

28. Saha O (2013) Investigation of the function of the LNX family of E3 ubiquitin ligases in the nervous system. PhD Thesis, University College Cork. https://cora.ucc.ie/handle/10468/1195

29. Petersen PH, Zou K, Hwang JK, Jan YN, Zhong W (2002) Progenitor cell maintenance requires numb and numblike during mouse neurogenesis. Nature 419:929–934

30. Zhong W, Feder JN, Jiang MM, Jan LY, Jan YN (1996) Asymmetric localization of a mammalian numb homolog during mouse cortical neurogenesis. Neuron 17:43–53

31. Klein AL, Zilian O, Suter U, Taylor V (2004) Murine numb regulates granule cell maturation in the cerebellum. Dev Biol 266:161–177

32. Shen Q, Zhong W, Jan YN, Temple S (2002) Asymmetric Numb distribution is critical for asymmetric cell division of mouse cerebral cortical stem cells and neuroblasts. Development 129:4843–4853

33. Zilian O, Saner C, Hagedorn L, Lee HY, Sauberli E, Suter U, Sommer L, Aguet M (2001) Multiple roles of mouse Numb in tuning developmental cell fates. Curr Biol 11:494–501

34. Zhong W, Jiang MM, Schonemann MD, Meneses JJ, Pedersen RA, Jan LY, Jan YN (2000) Mouse numb is an essential gene involved in cortical neurogenesis. Proc Natl Acad Sci U S A 97:6844–6849

35. Li HS et al (2003) Inactivation of Numb and Numblike in embryonic dorsal forebrain impairs neurogenesis and disrupts cortical morphogenesis. Neuron 40:1105–1118

36. Petersen PH, Zou K, Krauss S, Zhong W (2004) Continuing role for mouse Numb and Numbl in maintaining progenitor cells during cortical

neurogenesis. Nat Neurosci 7:803–811

37. Rasin MR et al (2007) Numb and Numbl are required for maintenance of cadherin-based adhesion and polarity of neural progenitors. Nat Neurosci 10:819–827

38. Butler K, Martinez LA, Tejada-Simon MV (2013) Impaired cognitive function and reduced anxiety-related behavior in a promyelocytic leukemia (PML) tumor suppressor protein-deficient mouse. Genes Brain Behav 12:189–202

39. Semenova S, Contet C, Roberts AJ, Markou A (2012) Mice lacking the beta4 subunit of the nicotinic acetylcholine receptor show memory deficits, altered anxiety- and depression-like behavior, and diminished nicotine-induced analgesia. Nicotine Tob Res 14:1346–1355

40. Zhou L et al (2015) Numb deficiency in cerebellar Purkinje cells impairs synaptic expression of metabotropic glutamate receptor and motor coordination. Proc Natl Acad Sci U S A 112:15474–15479

41. Arroyo JD, Lee GM, Hahn WC (2008) Liprin alpha1 interacts with PP2A B56gamma. Cell Cycle 7:525–532

42. Liu YC et al (2014) The PPFIA1-PP2A protein complex promotes trafficking of Kif7 to the ciliary tip and Hedgehog signaling. Sci Signal 7:ra117

43. Higa S, Tokoro T, Inoue E, Kitajima I, Ohtsuka T (2007) The active zone protein CAST directly associates with Ligand-of-Numb protein X. Biochem Biophys Res Commun 354:686–692

44. Sudhof TC (2012) The presynaptic active zone. Neuron 75:11–25

45. Ko J, Na M, Kim S, Lee JR, Kim E (2003) Interaction of the ERC family of RIM-binding proteins with the liprin-alpha family of multidomain proteins. J Biol Chem 278:42377–42385

46. Nachat R, Cipolat S, Sevilla LM, Chhatriwala M, Groot KR, Watt FM (2009) KazrinE is a desmosome-associated liprin that colocalises with acetylated microtubules. J Cell Sci 122:4035–4041

47. Guerrier S et al (2009) The F-BAR domain of srGAP2 induces membrane protrusions required for neuronal migration and morphogenesis. Cell 138:990–1004

48. Charrier C et al (2012) Inhibition of SRGAP2 function by its human-specific paralogs induces neoteny during spine maturation. Cell 149:923–935

49. Dennis MY et al (2012) Evolution of human-specific neural SRGAP2 genes by incomplete segmental duplication. Cell 149:912–922

50. Ma Y, Mi YJ, Dai YK, Fu HL, Cui DX, Jin WL (2013) The inverse F-BAR domain protein srGAP2 acts through srGAP3 to modulate neuronal differentiation and neurite outgrowth of mouse neuroblastoma cells. PLoS One 8:e57865

51. Coyle IP, Koh YH, Lee WC, Slind J, Fergestad T, Littleton JT, Ganetzky B (2004) Nervous wreck, an SH3 adaptor protein that interacts with Wsp, regulates synaptic growth in Drosophila. Neuron 41:521–534

52. Ro H, Dawid IB (2009) Organizer restriction through modulation of Bozozok stability by the E3 ubiquitin ligase Lnx-like. Nat Cell Biol 11:1121–1127

53. Ro H, Dawid IB (2010) Lnx-2b restricts gsc expression to the dorsal mesoderm by limiting nodal and Bozozok activity. Biochem Biophys Res Commun 402:626–630

54. Ro H, Dawid IB (2011) Modulation of Tcf3 repressor complex composition regulates cdx4 expression in zebrafish. EMBO J 30:2894–2907